

ABSTRACT

Title of Thesis: FLUXOMIC EVALUATION OF BOVINE
EMBRYO NUTRIENT UTILIZATION

Robert Clifford, Master of Science, 2017

Thesis Directed By: Professor Ganesh Sriram, Department of
Chemical and Biomolecular Engineering

One of the main factors that influence the success of embryo production is the culture medium that is used for embryo incubation. The nutritional diet composition can result in altered epigenetics that can negatively affect the health of the resulting offspring. This study focused on investigating the influence of medium components on the metabolic identity of the bovine embryo. This goal was accomplished by using a ^{13}C labeling that can be detected with a mass spectrometer. The ^{13}C was initially provided in the form of a simple sugar that was later converted into lactic acid by the bovine embryo. The presence of fully labeled lactic acid after incubation demonstrated that the bovine embryo utilizes the aerobic glycolysis pathway for some energy generation. This pathway was shown to be used to a greater extent when glucose was the only simple sugar provided to the embryo compared to fructose.

FLUXOMIC EVALUATION OF BOVINE EMBRYO NUTRIENT UTILIZATION

By

Robert Clifford

Thesis submitted to the Faculty of the Graduate School of the
University of Maryland, College Park, in partial fulfillment
of the requirements for the degree of
Master of Science

2017

Advisory Committee

Dr. Ganesh Sriram, Chair

Dr. Nam Sun Wang

Dr. Amy Karlsson

Dr. Carol Keefer

© Copyright by
Robert Clifford
2017

Acknowledgments

I would like to thank the University of Maryland for fulfilling my dream of being a student in this illustrious university. I would also like to thank my committee of Dr. Ganesh Sriram, Dr. Nam Sun Wang, Dr. Amy Karlsson and Dr. Carol Keefer for your assistance throughout this process. I would also like to thank my fellow lab colleagues for helping out my experiments. Most importantly, I would like to thank my parents for supporting me at every point and not letting me give up.

Table of Contents

Acknowledgments	ii
Table of Contents	iii
Chapter 1 Historical Background	1
Chapter 2 Technical Background	4
2.1 Instrumentation	4
2.2 Derivatization of Metabolites	9
2.3 Metabolic Flux Analysis	14
2.4 Label Based Metabolic Flux Analysis	20
Chapter 3 Experimental Results	35
3.1 Spent Culture Medium Analysis	35
3.2 Fluxomic Evaluation	49
Chapter 4 Conclusions	63
Chapter 5 Experiment Methods	64
5.1 Bovine Embryo Cell Growth	64
5.2 Isotope Labeling Experiment	64
5.3 Fluxomic Evaluation from Isotopomer Data	65
Supplementary Information	66
List of Figures	67
Bibliography	70

Chapter 1: Historical Background

Due to increasing demand for meat and milk production, embryo transfer in the cattle industry is a growing business. Mammalian embryos also play an important role in scientific research as a powerful model for human fertility and development (Perkel 2015). Despite decades of research, current embryo production protocols are not as optimal as demonstrated by poorer embryo quality, aberrant embryo metabolism, and lower pregnancy rates observed with in vitro produced embryos as compared to their in vivo counterparts (Lonergan 2008). Pregnancy rates for in vitro compared to in vivo produced bovine embryos is 10 to 20% lower (Singh 2007).

There is also evidence that the culture can result in altered epigenetics and gene expression which can detrimentally affect the health of the resulting offspring and cause a problem called large offspring syndrome (European 2010). This syndrome can be very problematic because the resulting offspring is larger than normal causing breathing difficulties, reluctance to suckle, cerebral dysplasia, increased prenatal losses and other difficulties due to altered energy metabolism (Chen). Little is known about the nutritional or metabolic requirements during early embryonic development. As assisted reproductive technologies have emerged as useful tools in the breeding of animals and for treatment of infertility, a more complete understanding of the essential metabolic pathways during preimplantation development will assist in developing culture systems and procedures that support normal embryonic and fetal development.

Understanding the metabolic basis of normal early embryo development will provide significant benefits to human and animal reproductive health. This research focused on the bovine embryo

incubated to form a structure called the blastocyst. The blastocyst structure is formed during cell division to create an outer shell of cells called trophoblasts and an inner mass of cells called embryoblasts. This stage is important because it is the last stage before implantation and critical to the success of the resulting offspring. The implantation is critical to the survival of the embryo because this is when the embryo and mother form a connection that remains throughout pregnancy (Prenatal Development 2013).

Theories regarding the delicate balance between bioenergetics and biosynthesis suggest an important role for glycolytic pathway components. More specifically, enzymes within the glycolytic pathway including glyceraldehyde 3-phosphate dehydrogenase and pyruvate kinase have shown to be used for the regulation of cell signaling, cell proliferation, lineage differentiation and apoptosis (Chang 2013 and Mazurek 2011). One example of this importance is shown when the enzyme glyceraldehyde 3-phosphate dehydrogenase has been shown in T-cells to binds to the messenger RNA that creates the compound called interferon gamma (Nicholss 2012). This suggests that the glycolysis pathway closely related to regulating interferon secretion. One study found that mice with an interferon knockout were not able to initiate normal pregnancy (Ashkar 2000). All of these are potentially significant in the creation of a competent embryo.

To date, studies focused on embryo metabolism have covered indirect means to measure glycolysis (Leese). The research covered in this thesis will take a more direct approach by combining metabolomics and fluxomic analysis to explore the glycolytic pathway. The first tool

of metabolomics provides a snapshot of the metabolic composition within a system, while fluxomics utilizes this tool to gather information of the metabolic pathways. To date, fluxomics has not been applied in the investigation of embryos. These applications will allow the establishment of a foundational base of knowledge and techniques to study the influence of nutritional strategies and environmental stressors on the embryo. One particular nutritional strategy that is examined in this research is the type of sugar supplied to the embryo before implantation. The commonly used sugar glucose has been found to be problematic for incorporation with the embryo. Some research have supported its use while other have claimed that it can be detrimental to the embryo and resulting offspring's health (Bernejo-Alvarez 2012 and Kimura 2004). One paper suggests that the incorporation of another sugar called fructose alongside glucose could be beneficial for a mammalian embryo (Tsuji 2009). Because of the problematic nature of the sugars supplied to embryo, this research focuses on providing different types of sugars to measure the resulting shift in metabolism associated.

Chapter 2: Technical Background

2.1 Instrumentation

A powerful analytical technique that is utilized by this project is mass spectrometry. This technique is used to analyze and separate various ions based on their mass to charge ratio. The ions that were analyzed can be separated by various types of mass spectrometers. The type of mass spectrometer that was used to separate these ions is called a quadrupole mass analyzer. This particular type of mass analyzer has four sets of parallel cylindrical rods that are arranged in a square formation. A voltage consisting of a DC and AC portion is applied to the rods to create an electrical field between the parallel rods. This electrical field is used to cause incoming ions to be set on a helical trajectory through the parallel rods. If the ions go through the parallel rods with a stable trajectory then the ions reach the mass detector where a resulting signal is produced by an electron multiplier. On the other hand, if the ions have an unstable trajectory due to strong or weak attraction or repulsion to the rods then the ions are discharged to the rods or the surrounding surface and thus will not reach the mass detector to produce a signal (Quadrupole 2017). The following equations are used to determine the trajectory of the ions in the mass spectrometer:

$$\frac{d^2x}{dt^2} = -\left(\frac{m}{z}\right)^{-1} \cdot \frac{U+V\cos(\omega t)}{r_o^2} x \quad [1]$$

$$\frac{d^2y}{dt^2} = -\left(\frac{m}{z}\right)^{-1} \cdot \frac{U+V\cos(\omega t)}{r_o^2} y \quad [2]$$

where x and y are directions perpendicular to the parallel rods, t is the time, r_o is half the distance between two opposing rods, U is the DC voltage applied, V is the AC voltage applied, ω is the

frequency of the alternating voltage, m is the molecular mass of the ion and z is the charge of the ion (Douglas 2009). From these equations we can see that by controlling the alternating and direct current voltages applied to the parallel rods, we can specify ions of a particular mass to charge to proceed through the mass detector for analysis. An important aspect of the mass spectrometer that is highlighted in these equations is that the compounds that are analyzed have to contain a charge. Uncharged molecules would not be influenced by the electrical field and would thus not have the trajectory needed to reach the mass detector. Since the compounds of interest are generally uncharged molecules, an ionization method is needed to create ions that can be analyzed. The ionization method used is called electron impact ionization. This method takes advantage of the following gas phase reaction:



where M is the molecule being ionized, e^{-} is an electron and M^{+} is the resulting cation (Märk 1985). The resulting cation also becomes susceptible to fragmentation to become a more stable molecule. This experiment utilized a Varian 300 mass spectrometer, which ionized samples using this reaction. Although the mass spectrometer is a powerful instrument, it is rarely used by itself. The reason is if the spectrometer is given several analyzable compounds at once the sensitivity is dramatically reduced as the spectrometer is forced to deal with more ions. Thus a particular technique called chromatography is commonly used to separate compounds before the spectrometer. The specific type of chromatography that was used in this experiment was gas chromatography using a Bruker 450 gas chromatograph. Gas chromatography separates these chemicals that can be vaporized into the gas phase without chemical deposition. Once in the gas phase the components are separated by utilizing two phases. One of these phases called the mobile phase or carrier gas. The carrier gas used for this experiment, helium, is an inert gas that

can push the newly vaporized ions through the system. The separation comes from the second phase called the stationary phase. The column is packed with inert solids that are coated. The separation is caused by the different strengths of physical and chemical interaction the vaporized ions have with this coating material. Ions that have stronger interactions with the coating material will more likely adsorb to the coating material and stay in the column longer (Poole 2012). Under the right conditions this separation allows enough time for the mass spectrometer to individually analyze each compound. This creates a gas chromatogram that produces peaks for each chemical that exits the column and enters the spectrometer (Figure 2.1).

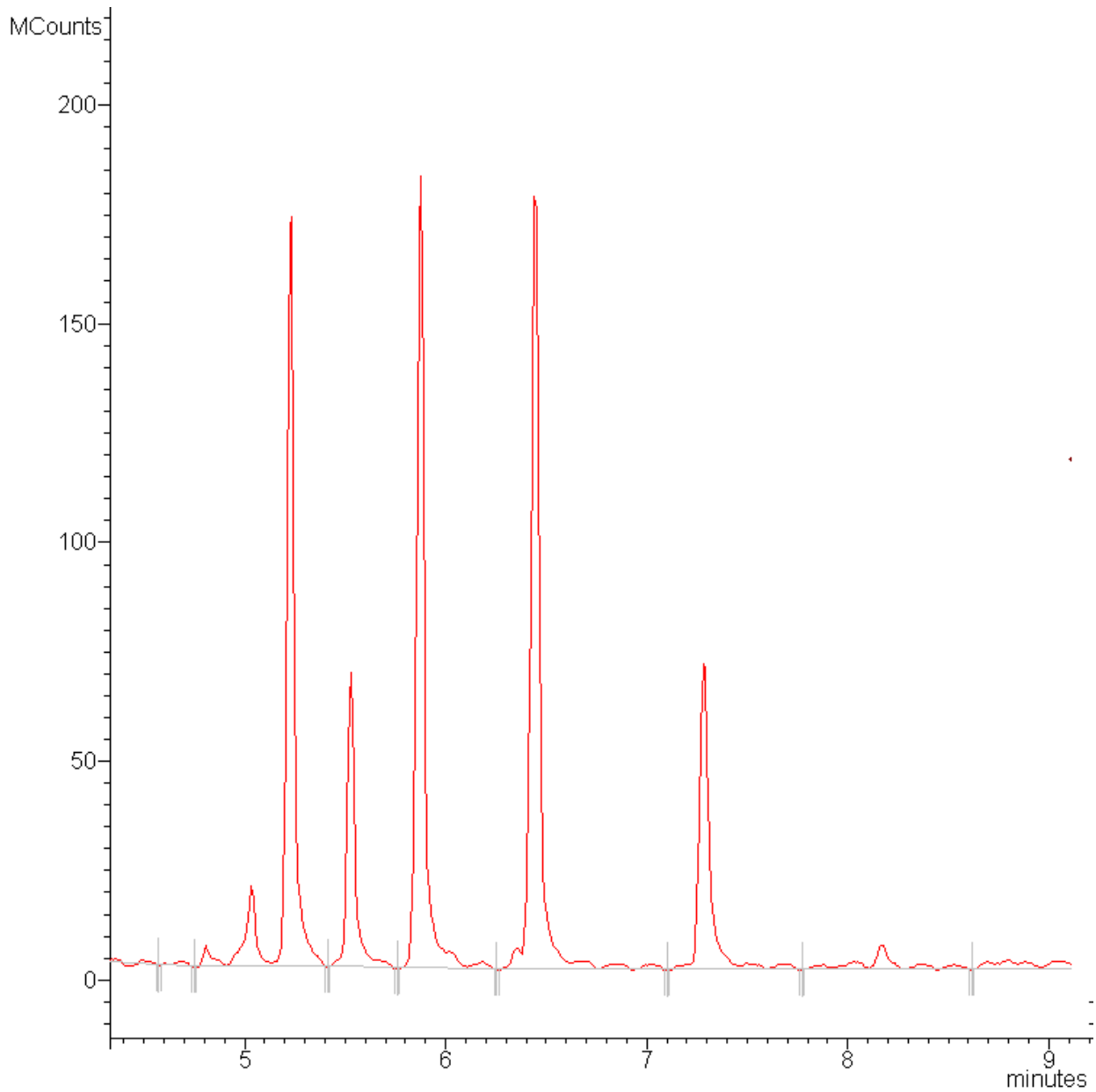


Figure 2.1 Example of a Gas Chromatogram

Gas chromatogram of culture medium used for bovine embryo incubation. The x-axis represents the amount of time each unknown chemical spent in the column before entering the spectrometer and the y-axis represents the amount of ions that are detected in this point of the experiment.

Just by looking at the chromatogram alone, it is impossible to determine the actual identity of the chemicals that are represented in each peaks. To help identify these chemicals it is helpful to look at a graph called a mass spectrum. Each of the peaks represented in Figure 2.1 is the accumulation of the ions that are detected by the mass spectrometer at each time point. The mass spectrum looks at the molecular weight of each ion created in the spectrometer (Figure 2.2).

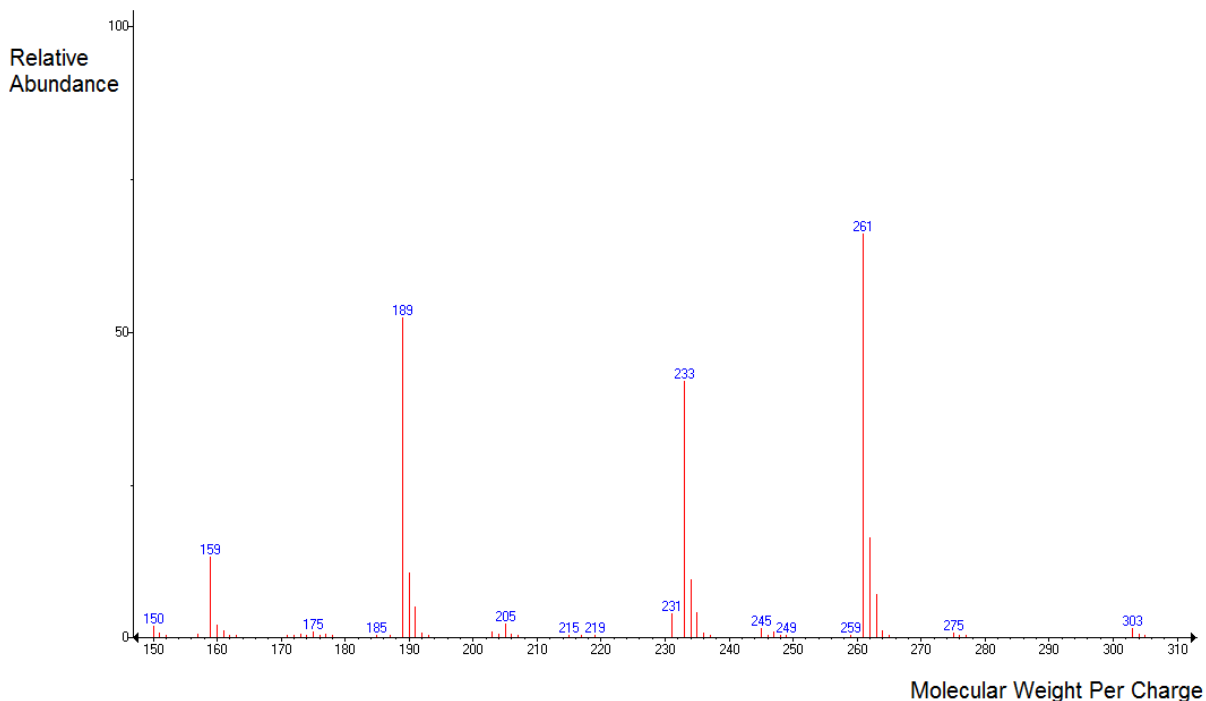


Figure 2.2 Example of a Mass Spectrum

Mass spectrum of one compound detected in the culture medium of the bovine embryo. The x-axis represents the molecular weight of the ions detected by the mass spectrometer and the y-axis represents the relative abundance of each ion detected.

Even though multiple ions are detected, all the major ions of this mass spectrum all originate from the same compound. This is because the fragmentation in the mass spectrometer mentioned

earlier in this sections can be used to create lower molecular weight ions from the same compound. To actually determine the exact identity of the compound that created this ion we need to specify the mechanism that created the ion.

2.2 Derivatization of Metabolites

For this particular experiment the goal was to study the intermediates and products of the metabolism of embryonic cells. These compounds are called metabolites and are important in providing information on the reaction pathways that are being utilized by the embryonic cells. The problem with these low molecular weight metabolites is that by themselves they are not volatile enough for analysis using a gas chromatogram. A powerful derivatizing agent is required to convert these metabolites into suitable compounds for analysis without altering or disrupting the carbons that I wished to investigate. Among the various derivatizing reaction that were available, the silylation reaction was useful due to the fact that silyl derivatives give favorable diagnostic fragmentation patterns from electron impact ionization (Silylation 2017). The silylating agent N-methyl-N-tert-butyldimethyl-silyl trifluoroacetamide was useful in converting the desired metabolites into compounds that could be examined using a gas chromatograph. This conclusion came from a paper by Xiaodon Huang and Fred E. Regneir that stated that this derivatizing agent was at least 10,000 times more hydrolytically stable than the more common trimethylsilyl derivative for analysis of key metabolites (Huang 2008). This was a very important aspect in considering derivatizing agents because it is important to keep the metabolites derivatized to maximize the conversion of compounds into volatile species since only a small amount of metabolites utilized by the embryonic cells. This derivatization can be used on many

functional groups including hydroxyl, carboxylic acid, amine, thiol and phosphate groups (Figure 2.3).

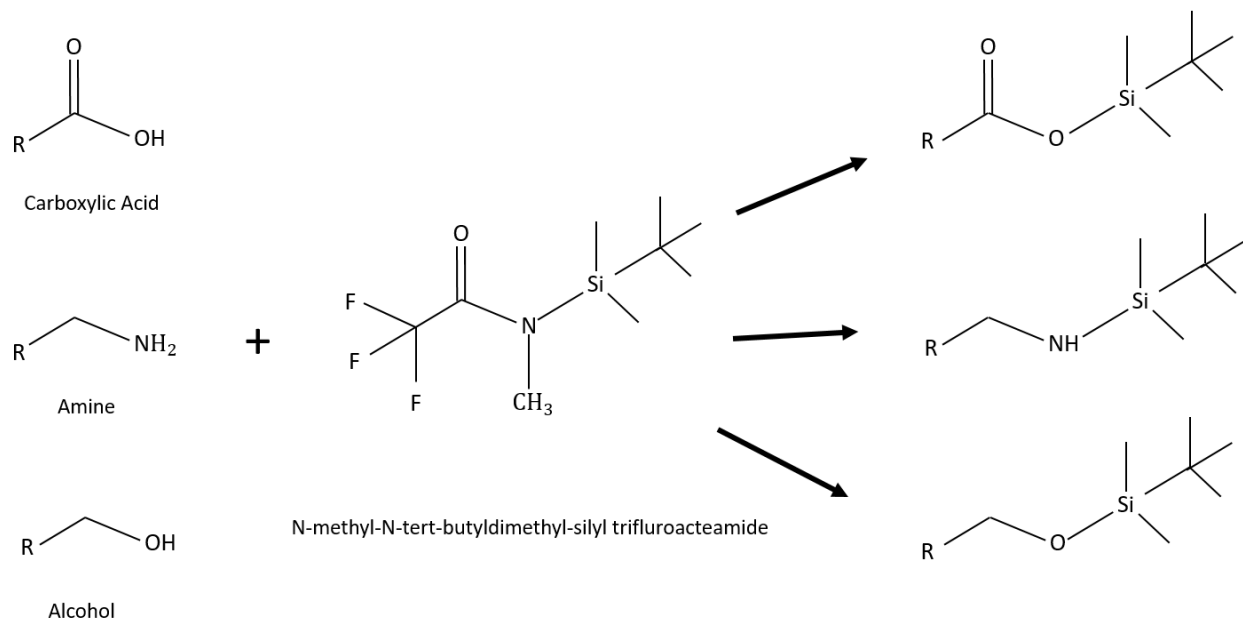


Figure 2.3 Silylation Derivatization Reaction for Gas Chromatography Utilization

Derivatization reaction to introduce a silyl group to make liquid phase molecules more volatile.

After deciding on the derivatization method used to help the analysis of these metabolites, the next step was to determine the optimal conditions that facilitated this reaction. The silylation reaction requires anhydrous conditions, thus anhydrous DMF was used as a solvent to dissolve the metabolites of interest (Villas Bôas 2011). Samples were also put through a freeze-drying process known as lyophilization to ensure that no water was available to disrupt the silylation reaction. This reaction is also suggested to be coupled with a reaction called oximation, which allows a milder derivatization (Yu). The oximation reaction converts aldehydes into more stable oximes (Figure 2.4).

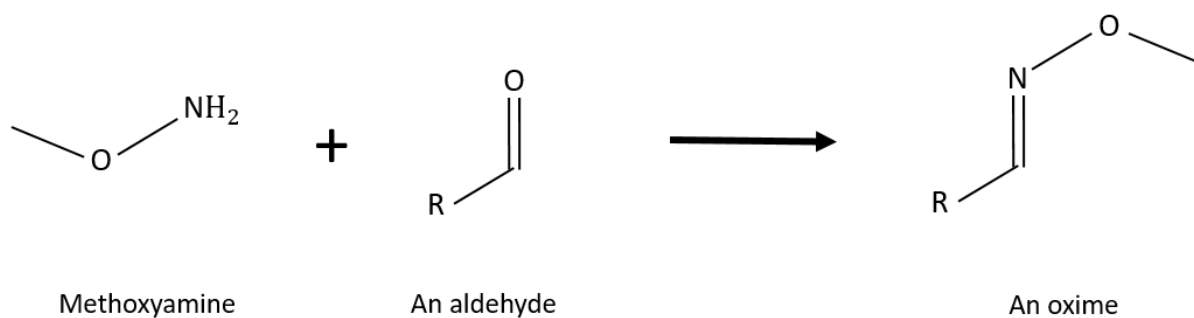


Figure 2.4 Methoximation Reaction

Derivatization reaction to convert aldehydes in oximes.

This reaction is accomplished by adding a compound called methoxyamine hydrochloride to our anhydrous solvent. This newly formed solvent is used to dissolve the metabolites of interest. With the metabolites dissolved, the new solution is heated at 70 degrees Celsius for 1.5 hours to facilitate the derivatization reactions. These two derivatization reactions were used on metabolites of interest for this experiment to produce a gas chromatogram and mass spectrum shown in Figure 2.1 and 2.2 of Section 2.1. With these derivatization reactions in mind, the actual ions could be identified by using mass spectrums to compare the produced ions with the theoretical molecular weight of the ions produced via these reactions (Figure 2.5).

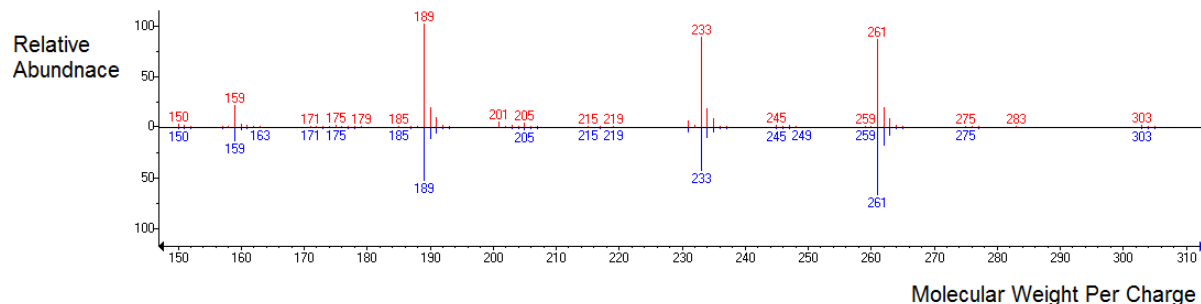


Figure 2.5 Comparing Experimental and Theoretical Mass Spectrums

Mass spectrum to identify a compound detected in the culture medium of the bovine embryo.

The x-axis represents the molecular weight of the ions detected by the mass spectrometer and the y-axis represents the relative abundance of each ion detected. The top spectrum represents a mass spectrum detected by the mass spectrometer and the bottom spectrum represents a theoretical mass spectrum for a lactic acid ion created using the silylation derivatization reaction.

The similarity between the theoretical spectrum and the experimental spectrum confirm the identity of this peak to be lactic acid. Using this idea, peaks on the gas chromatogram can be identified (Figure 2.6).

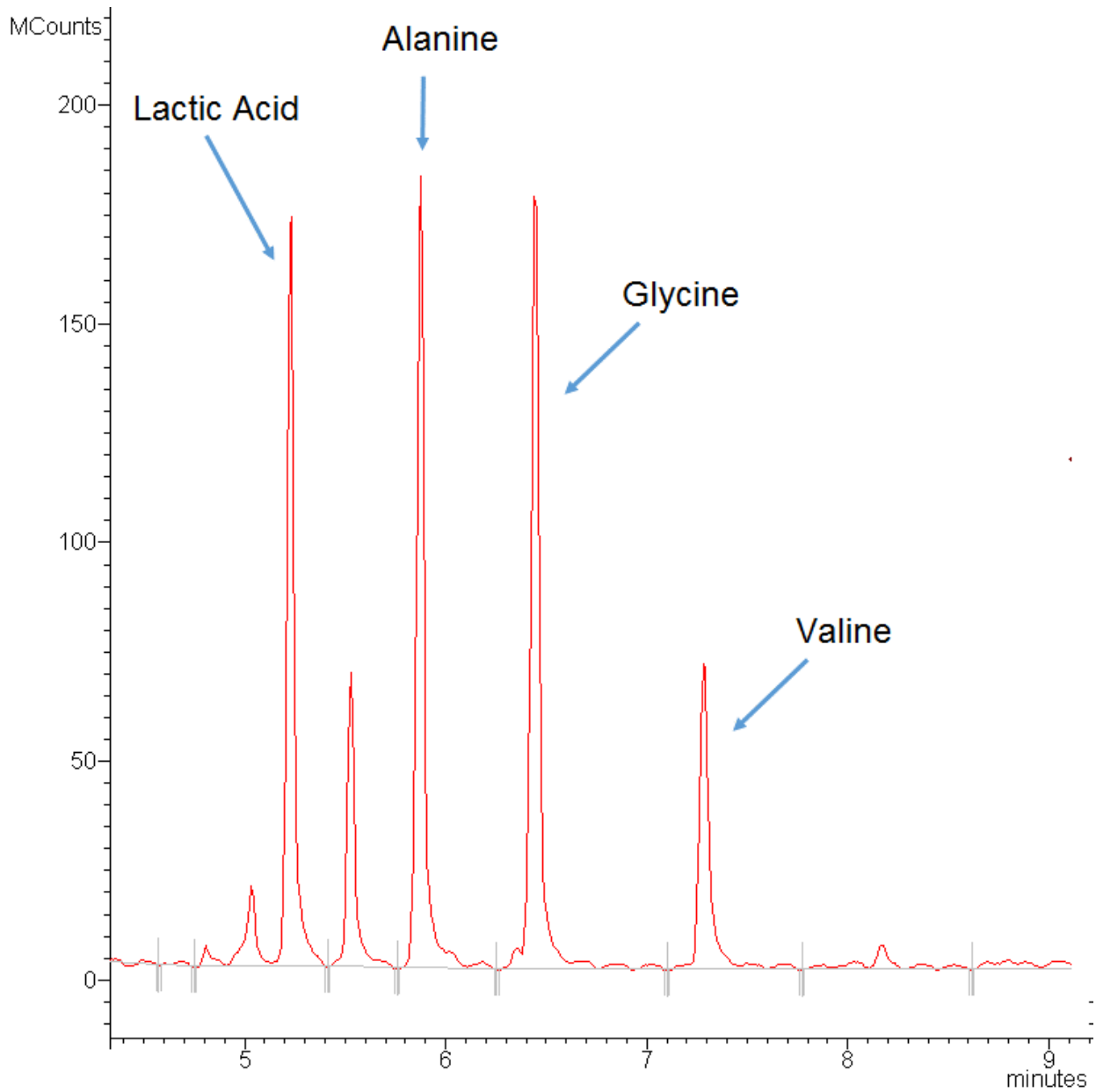


Figure 2.6 Example of a Gas Chromatogram with Labeled Peaks

Gas chromatogram of culture medium used for bovine embryo incubation with peaks labeled with the corresponding compound that produced the peak. The x-axis represents the amount of time each unknown chemical spent in the column before entering the spectrometer and the y-axis represents the amount of ions that are detected in this point of the experiment.

2.3 Metabolic Flux Analysis

Metabolic Flux Analysis is an analytical technique that has been utilized to gain a better understanding of various cells throughout the years (Nikel and Sauer 2006). This technique falls under the field of study known as fluxomics. The goal of a fluxomic study is to develop a better understanding of the rates of reactions utilized by the cell of interest. This information can be important in creating future studies with the goal of manipulating the cell to behave a certain way by controlling these rates of reactions. Metabolic flux analysis accomplishes this goal by creating a mathematical model that simulates rates of reactions used in the cell. The mathematical model is populated with reactions that complete the metabolic network utilized by mammalian cells. This network was completed with reactions that were taken from the website HumanCyc (HumanCyc 2017). The website contains information on the substrate and products used in each reaction for human cells. Since both human and bovine cells are mammalian, the reactions taken from this website were assumed to be utilized by the bovine embryo. The website also has information on the rearrangement of elements from the conversion of compounds. Although the cell has many reactions, this section will explain the details of metabolic flux analysis using a smaller model network shown below to gain a better understanding of the math involved for this research (Figure 2.7).

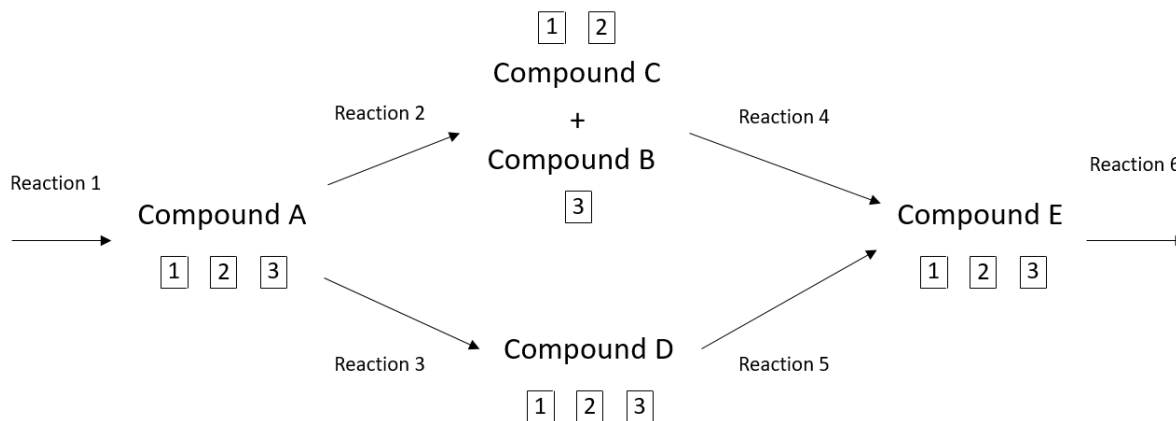


Figure 2.7 Sample Metabolic Network

Theoretical model to show the creation and consumption of compounds via metabolic reactions.

The sample model shown in Figure 2.7 is a theoretical model and can be replaced and expanded with real compounds and reactions. In this figure each compound is shown with boxed numbers to represent a specific element to track the flow of the elements throughout the metabolic network. In this figure, the arrows represent biological reactions to show the conversion of one compound into another compound. As mentioned earlier, the goal is to define and quantitate the rates of each reaction in the model. For a steady state system we find that the rate of reactions are dependent on other reactions. For example, the rate of reaction of reaction 1 will be the same as the rate of reaction 6. With this in mind, we find that we can define all the rates of reactions of an entire metabolic network by defining only a select amount of reactions. The total amount of reactions that can vary for a metabolic network is defined as the degree of freedom. This degree of freedom can be defined for different metabolic systems based on the following equation:

Degree of Freedom

$$\begin{aligned} &= \text{Number of Total Reactions} \\ &- \text{Number of Independent Intracellular Metabolites} \\ &- \text{Number of Measured Reactions} \end{aligned} \quad [4]$$

Equation 4 is used to calculate a degree of freedom of 2 variable reaction for Figure 2.3 since we are working with 6 total reaction and 4 independent intracellular metabolites (since Compound B and C are dependent on each other). As indicated by equation 4, if some reactions can be measured then the total amount of variable reactions can be reduced by the total amount of measured reactions. For the case of Figure 2.7, an example is by defining the rate of reaction 1 as 100 moles per second and rate of reaction 2 as 40 moles per second leads to simple calculations that can be used to define the rest of the rates of reactions (rate of reaction 6 = 100 moles per second, rate of reaction 4 = 40 moles per second and rate of reactions 3 and 5 = 60 moles per second). Although this example requires basic math to provide the final rates of reactions, a bigger metabolic network requires a more systematic approach to calculate the final rates. For a steady state system, the following equation is employed for defining the influence of reaction rates on the production and consumption of metabolites:

$$S \cdot v = 0 \quad [5]$$

where S represents a stoichiometric matrix used to define the production and consumption of individual compounds by each reaction and v represents the values of each reaction rate in the metabolic network. Each columns of the S matrix represents each reaction in the metabolic network, while on the other hand each row represents each compound in the network. An expanded view of the matrices shown in equation 5 representing Figure 2.7 can be created (Figure 2.8).

	Reaction 1	Reaction 2	Reaction 3	Reaction 4	Reaction 5	Reaction 6
Compound A	+1	-1	-1	0	0	0
Compound B	0	+1	0	-1	0	0
Compound C	0	+1	0	-1	0	0
Compound D	0	0	+1	0	-1	0
Compound E	0	0	0	+1	+1	-1

Rate of Reaction 1
Rate of Reaction 2
Rate of Reaction 3
Rate of Reaction 4
Rate of Reaction 5
Rate of Reaction 6

• = 0

Figure 2.8 Sample Matrix for Compound Balancing

Matrix equation based on equation 5 used to associate the consumption and generation of compounds with the reactions in Figure 2.7.

For equation 5 and Figure 2.8 to be useable we break down each matrix into two components depending on the type of reactions to give the following equation:

$$S_x \cdot v_x + S_m \cdot v_m = 0 \quad [6]$$

where v_x represents the value of the dependent reaction rates, v_m represents the values of the measured and variable reaction rates, S_x represents the portion of the stoichiometric matrix dealing with production and consumption of individual compounds that is only concerned with dependent reaction rates and S_m represents the portion of the stoichiometric matrix that is only

concerned with variable and measured reaction rates. This equation can be utilized for metabolic networks like the one shown in Figure 2.7 to create a matrix equation (Figure 2.9).

	Reaction 3	Reaction 4	Reaction 5	Reaction 6		Reaction 1	Reaction 2		
Compound A	-1	0	0	0	•	Compound A	+1	-1	•
Compound B	0	-1	0	0		Compound B	0	+1	
Compound C	0	-1	0	0		Compound C	0	+1	
Compound D	+1	0	-1	0		Compound D	0	0	
Compound E	0	+1	+1	-1		Compound E	0	0	
	S_x				+		S_m		= 0
				Rate of Reaction 3	•			Rate of Reaction 1	•
				Rate of Reaction 4	+			Rate of Reaction 2	•
				Rate of Reaction 5	+				•
				Rate of Reaction 6	+				•
				v_x	+			v_m	= 0

Figure 2.9 Separated Sample Matrix for Compound Balancing

Separated matrix equation based on equation 6 used to associate the consumption and generation of compounds with the reactions in Figure 2.7. Reactions 1 and 2 are defined as the variable or measured reactions. v_x represents the value of the dependent reaction rates, v_m represents the values of the measured and variable reaction rates, S_x represents the portion of the stoichiometric matrix dealing with production and consumption of individual compounds that is only concerned with dependent reaction rates and S_m represents the portion of the stoichiometric matrix that is only concerned with variable and measured reaction rates.

For each metabolic network there exist many possible combinations for the variable reactions used, but for this case we will stick with reactions 1 and 2. Equation 5 and Figure 2.9 can be completely solved when dependent reaction rates are defined.

These equation can be solved for the specific case mentioned on page 16, where the reaction rates 1 and 2 are defined as 100 and 40 moles per second respectively (Figure 2.10).

	Reaction	Reaction	Reaction	Reaction		Reaction	Reaction						
	3	4	5	6		1	2						
Compound A	-1	0	0	0	•	60 moles/sec Reaction 3	+	Compound A	+1	-1	•	=	0
Compound B	0	-1	0	0		40 moles/sec Reaction 4		Compound B	0	+1			
Compound C	0	-1	0	0		60 moles/sec Reaction 5		Compound C	0	+1			
Compound D	+1	0	-1	0		100 moles/sec Reaction 6		Compound D	0	0			
Compound E	0	+1	+1	-1		100 moles/sec Reaction 1		Compound E	0	0			
	S_x					v_x		S_m		v_m			

Figure 2.10 Calculating Dependent Reaction Rates

Matrix equation based on equation 6 to calculate dependent reaction rates from the metabolic system given in Figure 2.7. Reactions 1 and 2 are defined as the variable or measured reactions. v_x represents the value of the dependent reaction rates, v_m represents the values of the measured and variable reaction rates, S_x represents the portion of the stoichiometric matrix dealing with production and consumption of individual compounds that is only concerned with dependent reaction rates and S_m represents the portion of the stoichiometric matrix that is only concerned with variable and measured reaction rates.

As we can see in Figure 2.10, the results of this matrix mathematics leads to the same reaction rates mentioned in page 16. As mentioned earlier, this matrix math can be used for bigger metabolic networks to calculate the dependent reaction rates when the independent reaction rates

are defined. Now that the reaction rates can be defined for the entire metabolic network when the independent reaction rates are defined, the next steps is figuring out a way to determine the actual values of these variable reaction rates.

2.4 Label Based Metabolic Flux Analysis

As mentioned in Section 2.3, defining a metabolic system requires compiling reaction rates used by an organism and then quantifying the rates of these reactions. The challenge of the metabolic flux analysis is determining the actual values of the variable reaction rates that are used to help specify the position of the metabolic network completely. One method that allows direct analysis for interpretation of reaction rates takes advantage of a label-based approach. This is done by labeling a substrate that is fed to the organism. The label must be able to remain intact after the various reactions that take place within the organism. The amount of labeling must also be easily detected in the different compounds that are produced via the metabolic network. Once the labeled substrate is given enough time during incubation of the organism to be incorporated into the metabolic network and converted into metabolites, the goal is to examine the compounds with the label to gain a better understanding of the metabolic network used by the organism. Just like in Section 2.3, the use of a smaller metabolic network will be used to explain the science. This sample metabolic network is similar to Figure 2.7, but with two options for each atom in this metabolic network (Figure 2.11).

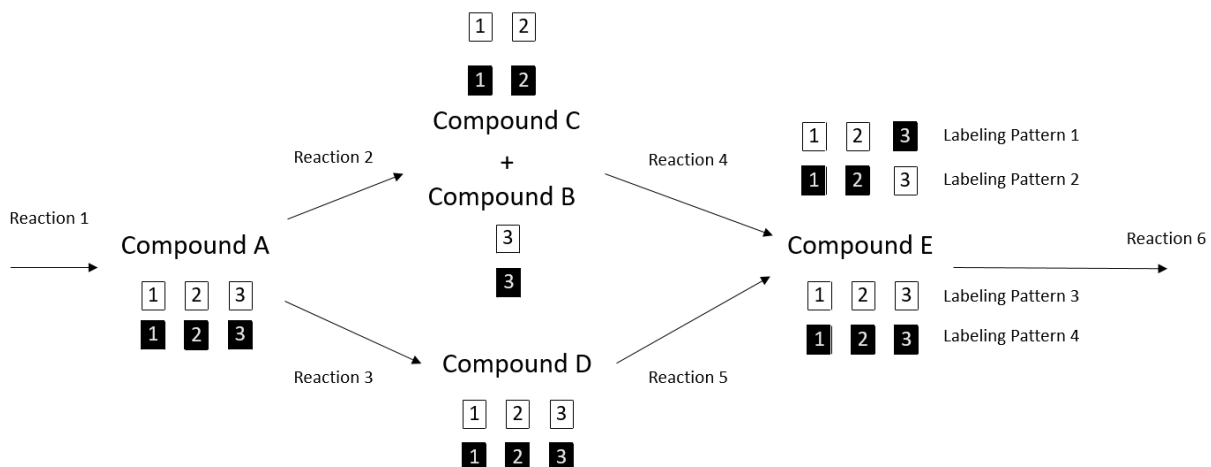


Figure 2.11 Sample Metabolic Network with Labeling Patterns

Theoretical model to show the creation and consumption of compounds with specific labeling patterns via metabolic reactions. Each horizontal set of boxed number represents a compound with a specific labeling pattern. A black background and white text is defined as being atoms that are labeled and a white background and black text are defined as atoms being unlabeled.

The substrate for this figure is provided as either being a fully unlabeled three atom substrate or a fully labeled three atom substrate. Although the example given has a specific configuration of either fully labeled or unlabeled, there are multiple configurations that can be used including partially labeled species for different information. Once the substrate is incorporated into the model as compound A, the organism has two options on how it will choose to use this compound. The first option, reaction 3, will leave the three elements together. On the other hand the second option, reaction 2, will break the three element compound into two compounds with labeling incorporated in both the compounds. The extent to which each option is used by the organism is one of the variable reaction rates mentioned earlier in this paper. These variable

reaction rates are important because they eventually create different labeling patterns in the final metabolite of this metabolic network. The first reaction pathway, reaction 3 and then reaction 5, will create compound E with labeling patterns 3 and 4 shown in Figure 2.11. These labeling patterns are the same options as the labeling patterns of the original compound A since the elements remain together throughout the reaction pathway. The second reaction pathway, reactions 2 and then reaction 4, create compound E with more labeling patterns than the other reaction pathway. Compound E is created with labeling patterns 1 through 4 instead of just labeling patterns 3 and 4. The reason is reaction 2 breaks down compound A into two species which can be recombined in reaction 4 using elements from other substrate. When recombining the elements in reaction 4, the organism will not preferentially choose to use elements originating from the same substrate. This allows the compound E to be partially labeled instead of fully unlabeled and labeled. By examining the labeling patterns of compound E we can predict the variable reaction rates since different reaction rates will cause different ratios of the labeling patterns used above. For example in Figure 2.11, if the substrate is fed with 50 % fully labeled substrate and 50 % fully unlabeled substrate and the reaction rates of 2 and 3 are identical then the ratio of labeling patterns 1, 2, 3 and 4 will be 12.5 %, 12.5 %, 25 % and 25 % respectively. When given an example where we can detect the labeling pattern ratios we can guess the variable reaction rates and check the resulting labeling to predict the state of organism studied. Although this specific example allows direct calculation of the reaction rates, more complicated metabolic networks with more variable reaction rates require a systematic approach to the predictions. A concept that was used to simplify the reaction rate calculations is called cumomer. This concept allows faster computation to predict the labeling patterns for specific metabolic states. The faster computation time is important because the larger metabolic network will have many variable

reaction rates that lead to a countless amount of possibilities that could explain the labeling pattern. The cumomer concept simplifies the calculations by defining each element as being in either two states. The two states are defined as 1 for being labeled and X for being either unlabeled or labeled. The state that can be either unlabeled or labeled is used to allow calculations without fully knowing the labeling pattern, which allows easier calculations. This designation creates labeling patterns of different orders depending on the amount of elements that are defined as labeled (Figure 2.12).

Three Atom Compound		
<div style="display: flex; justify-content: center; gap: 10px;"> 1 2 3 </div>		
Order 1 Cumomers	Order 2 Cumomers	Order 3 Cumomer
1XX	11X	111
X1X	1X1	
XX1	X11	

Figure 2.12 Cumomers System for a Three Atom Compound

Cumomer system defined for a three atom compound. Atoms defined as 1 are definitively labeled, while atoms defined as X are either labeled or unlabeled.

As you can imagine the amount of possible cumomers will rapidly increase when working with compounds of many atoms. The exact labeling pattern for a specific compound can be determined when the ratios of each cumomer is defined (Figure 2.13).

Three Atom Compound

1 2 3

Order 1 Cumomer Ratios

$$1XX = 0.3$$

$$X1X = 0.3$$

$$XX1 = 0.3$$

Order 2 Cumomer Ratios

$$11X = 0.3$$

$$1X1 = 0.3$$

$$X11 = 0.3$$

Order 3 Cumomer Ratio

$$111 = 0.3$$

Resulting Labeling Pattern Ratio

$$\boxed{1} \boxed{2} \boxed{3} = 0.7$$

$$\blacksquare 1 \blacksquare 2 \blacksquare 3 = 0.3$$

Figure 2.13 Determining Labeling Pattern from Cumomer Ratios for a Three Atom Compound

A specific of the cumomer system defined for a three atom compound. Atoms defined as 1 are definitively labeled, while atoms defined as X are either labeled or unlabeled. Each cumomer has a numerical value representing the ratio of each compound designated with the specific cumomer labeling pattern. A black background and white text is defined as being atoms that are labeled and a white background and black text are defined as atoms being unlabeled.

As shown in Figure 2.13, the only possible labeling pattern is 30 percent fully labeled and 70 percent fully unlabeled. This cumomer system that we defined can be used to define every metabolite in the metabolic network. By defining reaction rates for a metabolic network we can define the cumomer ratios for each metabolite, which then gives a specific labeling ratio. A

balance equation is useful to give a better understanding of the generation and consumption of these cumomers for the metabolic network shown in Figure 2.7 and 2.11 (Figure 2.14)

Cumomer Order	Cumomer of Interest	Generation of Cumomer	Consumption of Cumomer
Order 1 Cumomers	Compound A 1XX	$v1 \cdot \alpha$	$v2 \cdot A\ 1XX + v3 \cdot A1XX$
	Compound A X1X	$v1 \cdot \alpha$	$v2 \cdot A\ 1XX + v3 \cdot A1XX$
	Compound A XX1	$v1 \cdot \alpha$	$v2 \cdot A\ 1XX + v3 \cdot A1XX$
	Compound B 1	$v2 \cdot A\ XX1$	$v4 \cdot B\ 1$
	Compound C 1X	$v2 \cdot A\ 1XX$	$v4 \cdot C\ 1X$
	Compound C X1	$v2 \cdot A\ X1X$	$v4 \cdot C\ X1$
	Compound D 1XX	$v3 \cdot A\ 1XX$	$v5 \cdot D\ 1XX$
	Compound D X1X	$v3 \cdot A\ X1X$	$v5 \cdot D\ X1X$
	Compound D XX1	$v3 \cdot A\ XX1$	$v5 \cdot D\ XX1$
	Compound E 1XX	$v4 \cdot C\ 1X + v5 \cdot D\ 1XX$	$v6 \cdot E\ 1XX$
	Compound E X1X	$v4 \cdot C\ X1 + v5 \cdot D\ X1X$	$v6 \cdot E\ X1X$
Compound E XX1	$v4 \cdot B\ 1 + v5 \cdot D\ XX1$	$v6 \cdot E\ XX1$	
Order 2 Cumomers	Compound A 11X	$v1 \cdot \alpha$	$v2 \cdot A\ 11X + v3 \cdot A11X$
	Compound A 1X1	$v1 \cdot \alpha$	$v2 \cdot A\ 1X1 + v3 \cdot A1X1$
	Compound A X11	$v1 \cdot \alpha$	$v2 \cdot A\ X11 + v3 \cdot AX11$
	Compound C 11	$v2 \cdot A\ 11X$	$v4 \cdot C\ 11$
	Compound D 11X	$v3 \cdot A\ 11X$	$v5 \cdot D\ 11X$

	Compound D 1X1	$v_3 \cdot A_{1X1}$	$v_5 \cdot D_{1X1}$
	Compound D X11	$v_3 \cdot A_{X11}$	$v_5 \cdot D_{X11}$
	Compound E 11X	$v_4 \cdot C_{11} + v_5 \cdot D_{11X}$	$v_6 \cdot E_{11X}$
	Compound E 1X1	$v_4 \cdot C_{1X} \cdot B_1 + v_5 \cdot D_{1X1}$	$v_6 \cdot E_{1X1}$
	Compound E X11	$v_4 \cdot C_{X1} \cdot B_1 + v_5 \cdot D_{X11}$	$v_6 \cdot E_{X11}$
Order 3 Cumomers	Compound A 111	$v_1 \cdot \alpha$	$v_2 \cdot A_{111} + v_3 \cdot A_{111}$
	Compound D 111	$v_3 \cdot A_{111}$	$v_5 \cdot D_{111}$
	Compound E 111	$v_4 \cdot C_{11} \cdot B_1 + v_5 \cdot D_{111}$	$v_6 \cdot E_{111}$

Figure 2.14 Example of Cumomer Balances Arranged By Cumomer Order

Equations representing the generation and consumption of cumomers based on the metabolic network provided in Figure 2.7. $v_{\#}$ represents the reaction rate number based on Figure 2.7, E 1XX represents the cumomer 1XX from compound E and α represents the ratio of a substrate being fed into the network that is fully labeled.

The balances shown in Figure 2.14 shows how the reaction rates convert cumomers into other cumomers throughout the network. The reason Figures 2.12, 2.13 and 2.14 separate the cumomers based on order is that the calculations used to determine cumomers require individual calculations for each order starting with the lowest order cumomer. Starting with lower order cumomers is important because an important note seen in Figure 2.10 is that cumomer balances never deal with cumomers of a higher order than the cumomer of interest. The balances are used to calculate the actual values of the cumomers for specific reaction rates. This calculation starts

by arranging all the possible order 1 cumomers for every metabolite in the metabolic network into a matrix form (Figure 15).

	Compound A 1XX	Compound A X1X	Compound A XX1	Compound B 1	Compound C 1X	Compound C X1	Compound D 1XX	Compound D X1X	Compound D XX1	Compound E 1XX	Compound E X1X	Compound E XX1
Compound A 1XX												
Compound A X1X												
Compound A XX1												
Compound B 1												
Compound C 1X												
Compound C X1												
Compound D 1XX												
Compound D X1X												
Compound D XX1												
Compound E 1XX												
Compound E X1X												
Compound E XX1												

Figure 2.15 Example of Blank First Order Cumomer Matrix Arranged

Blank first order cumomer matrix that can be populated using the cumomer balance featured in Figure 2.10.

This matrix can then be populated using the cumomer balance featured in Figure 2.10 to help calculate the ratio for each cumomer. This blank matrix is used to create a generation and also a consumption matrix to help with the calculation Figure (2.16 and Figure 2.17).

	A 1XX	A X1X	A XX1	B 1	C 1X	C X1	D 1XX	D X1X	D XX1	E 1XX	E X1X	E XX1
A 1XX	v2+v3	0	0	0	0	0	0	0	0	0	0	0
A X1X	0	v2+v3	0	0	0	0	0	0	0	0	0	0
A XX1	0	0	v2+v3	0	0	0	0	0	0	0	0	0
B 1	0	0	0	v4	0	0	0	0	0	0	0	0
C 1X	0	0	0	0	v4	0	0	0	0	0	0	0
C X1	0	0	0	0	0	v4	0	0	0	0	0	0
D 1XX	0	0	0	0	0	0	v5	0	0	0	0	0
D X1X	0	0	0	0	0	0	0	v5	0	0	0	0
D XX1	0	0	0	0	0	0	0	0	v5	0	0	0
E 1XX	0	0	0	0	0	0	0	0	0	v6	0	0
E X1X	0	0	0	0	0	0	0	0	0	0	v6	0
E XX1	0	0	0	0	0	0	0	0	0	0	0	v6

Figure 2.16 Example of Generation Matrix for First Order Cumomers

Generation matrix for first order cumomers where the columns and rows represent the cumomers that are used as substrates for each individual reaction.

	A 1XX	A X1X	A XX1	B 1	C 1X	C X1	D 1XX	D X1X	D XX1	E 1XX	E X1X	E XX1
A 1XX	0	0	0	0	0	0	0	0	0	0	0	0
A X1X	0	0	0	0	0	0	0	0	0	0	0	0
A XX1	0	0	0	0	0	0	0	0	0	0	0	0
B 1	0	0	v2	0	0	0	0	0	0	0	0	0
C 1X	v2	0	0	0	0	0	0	0	0	0	0	0
C X1	0	v2	0	0	0	0	0	0	0	0	0	0
D 1XX	v3	0	0	0	0	0	0	0	0	0	0	0
D X1X	0	v3	0	0	0	0	0	0	0	0	0	0
D XX1	0	0	v3	0	0	0	0	0	0	0	0	0
E 1XX	0	0	0	0	v4	0	v5	0	0	0	0	0
E X1X	0	0	0	0	0	v4	0	v5	0	0	0	0
E XX1	0	0	0	v4	0	0	0	0	v5	0	0	0

Figure 2.17 Example of Consumption Matrix for First Order Cumomers

Consumption matrix for first order cumomers where the rows represent the cumomers that are the products generated from each reaction (cumomer of interest column in Figure 2.14) and the columns represent the substrate cumomers that are converted into the product cumomers by each reaction (consumption of cumomer column in Figure 2.14).

One reaction that is missing in both the generation and consumption reaction shown in Figure 2.15 and 2.16 is the initial reaction 1. This reaction is missing because there is no substrate cumomer that feeds this reaction. Reactions like reaction 1 are considered influxes as the substrate comes from the solution that is fed to the organism of interest. The ratio of labeled substrate is controlled by the experiment and is thus fixed. To account for influxes and other reactions that are accounted for in the generation matrix it is useful to add another matrix to complete the cumomer balance (Figure 2.18).

	A 1XX	A X1X	A XX1	B 1	C 1X	C X1	D 1XX	D X1X	D XX1	E 1XX	E X1X	E XX1
A 1XX	v2+v3	0	0	0	0	0	0	0	0	0	0	0
A X1X	0	v2+v3	0	0	0	0	0	0	0	0	0	0
A XX1	0	0	v2+v3	0	0	0	0	0	0	0	0	0
B 1	0	0	0	v4	0	0	0	0	0	0	0	0
C 1X	0	0	0	0	v4	0	0	0	0	0	0	0
C X1	0	0	0	0	0	v4	0	0	0	0	0	0
D 1XX	0	0	0	0	0	0	v5	0	0	0	0	0
D X1X	0	0	0	0	0	0	0	v5	0	0	0	0
D XX1	0	0	0	0	0	0	0	0	v5	0	0	0
E 1XX	0	0	0	0	0	0	0	0	0	v6	0	0
E X1X	0	0	0	0	0	0	0	0	0	0	v6	0
E XX1	0	0	0	0	0	0	0	0	0	0	0	v6

A 1XX
A X1X
A XX1
B 1
C 1X
C X1
D 1XX
D X1X
D XX1
E 1XX
E X1X
E XX1

A 1XX
A X1X
A XX1
B 1
C 1X
C X1
D 1XX
D X1X
D XX1
E 1XX
E X1X
E XX1

v1 • α
v1 • α
v1 • α
0
0
0
0
0
0
0
0
0
0
0

=

	A 1XX	A X1X	A XX1	B 1	C 1X	C X1	D 1XX	D X1X	D XX1	E 1XX	E X1X	E XX1
A 1XX	0	0	0	0	0	0	0	0	0	0	0	0
A X1X	0	0	0	0	0	0	0	0	0	0	0	0
A XX1	0	0	0	0	0	0	0	0	0	0	0	0
B 1	0	0	v2	0	0	0	0	0	0	0	0	0
C 1X	v2	0	0	0	0	0	0	0	0	0	0	0
C X1	0	v2	0	0	0	0	0	0	0	0	0	0
D 1XX	v3	0	0	0	0	0	0	0	0	0	0	0
D X1X	0	v3	0	0	0	0	0	0	0	0	0	0
D XX1	0	0	v3	0	0	0	0	0	0	0	0	0
E 1XX	0	0	0	0	v4	0	v5	0	0	0	0	0
E X1X	0	0	0	0	0	v4	0	v5	0	0	0	0
E XX1	0	0	0	v4	0	0	0	0	v5	0	0	0

Figure 2.18 Example of First Order Customer Balance in Matrix Form

The first 12x12 matrix represents the generation matrix, the second 12x12 matrix represents the consumption matrix, the first and third 12x1 matrix represents the customer ratios and the second 12x1 matrix represents influxes and other lower order customer expressions.

This expression provides a linear form that allows fast calculations. Once the values of the reactions rates are provided or estimated, the 12x12 matrices can be populated with numbers to allow simple calculation of the first order cumomer ratios represented in two of the 12x1 matrices provided. Once the first order cumomer ratios are defined, the next step is to do the same type of calculations for the second order cumomers (Figure 2.19).

	A 11X	A 1X1	A X11	C 11	D 11X	D 1X1	D X11	E 11X	E 1X1	E X11
A 11X	0	0	0	0	0	0	0	0	0	0
A 1X1	0	0	0	0	0	0	0	0	0	0
A X11	0	0	0	0	0	0	0	0	0	0
C 11	v2	0	0	0	0	0	0	0	0	0
D 11X	v3	0	0	0	0	0	0	0	0	0
D 1X1	0	v3	0	0	0	0	0	0	0	0
D X11	0	0	v3	0	0	0	0	0	0	0
E 11X	0	0	0	v4	v5	0	0	0	0	0
E 1X1	0	0	0	0	0	v5	0	0	0	0
E X11	0	0	0	0	0	0	v5	0	0	0

•

A 11X
A 1X1
A X11
C 11
D 11X
D 1X1
D X11
E 11X
E 1X1
E X11

+

A 11X	v1 • α
A 1X1	v1 • α
A X11	v1 • α
C 11	0
D 11X	0
D 1X1	0
D X11	0
E 11X	0
E 1X1	v4 • B1 + v4 • C1X
E X11	v4 • B1 + v4 • C1X

=

	A 11X	A 1X1	A X11	C 11	D 11X	D 1X1	D X11	E 11X	E 1X1	E X11
A 11X	v2+v3	0	0	0	0	0	0	0	0	0
A 1X1	0	v2+v3	0	0	0	0	0	0	0	0
A X11	0	0	v2+v3	0	0	0	0	0	0	0
C 11	0	0	0	v4	0	0	0	0	0	0
D 11X	0	0	0	0	v5	0	0	0	0	0
D 1X1	0	0	0	0	0	v5	0	0	0	0
D X11	0	0	0	0	0	0	v5	0	0	0
E 11X	0	0	0	0	0	0	0	v6	0	0
E 1X1	0	0	0	0	0	0	0	0	v6	0
E X11	0	0	0	0	0	0	0	0	0	v6

Figure 2.19 Example of Second Order Cumomer Balance in Matrix Form

The first 10x10 matrix represents the generation matrix, the second 10x10 matrix represents the consumption matrix, the first and third 10x1 matrix represents the cumomer ratios and the second 10x1 matrix represents influx reactions and the first order cumomers.

The second order cumomer balance contains two irregular cumomers that require special attention. The cumomers are E 1X1 and E XX1 because these second order cumomers can be

created by combining two first order cumomers in reaction 4. This forces the inclusion of this reaction along with the influx reaction in the second 10x1 matrix. Although this changes the equation, the process remains a simple linear calculation because at this point the first order cumomers are defined as a number from the previous calculation. The linear equation allows calculation of the second order cumomer ratios. With the second order cumomer ratios calculated, the next step is to do the same type of calculations for the higher order cumomers (Figure 2.20).

$$\begin{array}{c}
 \text{A } 111 \quad \text{D } 111 \quad \text{E } 111 \\
 \begin{array}{|c|c|c|}
 \hline
 0 & 0 & 0 \\
 \hline
 \text{v}3 & 0 & 0 \\
 \hline
 0 & \text{v}5 & 0 \\
 \hline
 \end{array}
 \cdot
 \begin{array}{|c|}
 \hline
 \text{A } 111 \\
 \hline
 \text{D } 111 \\
 \hline
 \text{E } 111 \\
 \hline
 \end{array}
 +
 \begin{array}{|c|}
 \hline
 \text{A } 111 \\
 \hline
 \text{D } 111 \\
 \hline
 \text{E } 111 \\
 \hline
 \end{array}
 \begin{array}{|c|}
 \hline
 \text{v}1 \cdot \alpha \\
 \hline
 0 \\
 \hline
 \text{v}4 \cdot \text{B}1 + \text{v}4 \cdot \text{C}11 \\
 \hline
 \end{array}
 =
 \begin{array}{c}
 \text{A } 111 \quad \text{D } 111 \quad \text{E } 111 \\
 \begin{array}{|c|c|c|}
 \hline
 \text{v}2+\text{v}3 & 0 & 0 \\
 \hline
 0 & \text{v}5 & 0 \\
 \hline
 0 & 0 & \text{v}6 \\
 \hline
 \end{array}
 \cdot
 \begin{array}{|c|}
 \hline
 \text{A } 111 \\
 \hline
 \text{D } 111 \\
 \hline
 \text{E } 111 \\
 \hline
 \end{array}
 \end{array}$$

Figure 2.20 Example of Third Order Cumomer Balance in Matrix Form

The first 3x3 matrix represents the generation matrix, the second 3x3 matrix represents the consumption matrix, the first and third 3x1 matrix represents the cumomer ratios and the second 3x1 matrix represents influx reactions and the first order cumomers.

This third order cumomer balance is the last balance for the sample metabolic network mentioned in this paper. With all the possible cumomer balances defined, all the cumomers for each metabolite can be calculated when reactions rates are set. As mentioned earlier, once all the cumomers are defined the exact labeling pattern can be defined for each metabolite in our network. This technique can be used to back calculate and estimate the reaction rates for an organism once the labeling pattern is identified. This is done by creating a program that continually creates cumomer profiles for different reaction rate conditions and comparing the

resulting profiles that are created. This program can take advantage of global optimizations to determine the reaction rates that most closely estimate the labeling pattern observed.

Chapter 3: Experimental Results

3.1 Spent Culture Medium Analysis

A desired analysis of a bovine embryo is one which allows a noninvasive approach. This approach is favorable for people working with in-vitro fertilization because it allows insight into the health and condition of the embryos without disrupting the embryo itself. Noninvasive analysis can also be helpful for research and development because it allows the embryo to remain intact for future experiments. For this particular experiment this analysis was achieved by focusing on the culture medium that contained the incubating embryo. Information can be gained from this medium because the embryo itself is emitting chemicals that can be analyzed by gas chromatography coupled with mass spectroscopy. Since mass spectroscopy detects molecular weight, this experiment takes advantage of working with isotopes that can be incorporated into the culture medium. The particular isotope used was carbon-13 because it is a stable isotope with a long half-life that can be used to follow carbon pathways of the embryos. Use of a labeled substrate would provide novel insight into the embryo's metabolism and nutrition. Before experiments were run, it was predicted that altering the type of substrates used could shift the carbon metabolism of the embryo. The substrate that was altered in this first experiment was the presence of either fructose or glucose in the embryo growth medium. Each embryo incubation contained the same amount of total ^{13}C to allow comparability studies between different culture conditions. The culture medium is taken after embryo incubation for mass spectrometry to determine the metabolic utilization of the labeled substrate. This spent medium will have ^{13}C labeling in different compounds depending on utilization of different metabolic pathways.

Before any experiments were run on the medium used to incubate the embryo, confirmation that the analytical methods taken advantage of are reliable was required to ensure accurate analysis. This was done by testing medium that was not used for incubation and spiked with various chemicals. This fresh medium was spiked with ^{13}C labeled versions of compounds potentially expected to be in the medium in future experiments. Along with the ^{13}C labeled chemicals, natural labeled version of these chemicals were provided to the fresh medium at different ratios to test the mass spectrometer's accuracy and resolution when discriminating between the labeled and unlabeled version of each chemical. The three variations of labeling in each compound being tested consisted of 50 percent ^{13}C labeled, 5 percent ^{13}C labeled, and 100 percent naturally labeled. Each of these variations were replicated 4 times to give a total of 12 samples to create calibration curves (Figure 3.1).

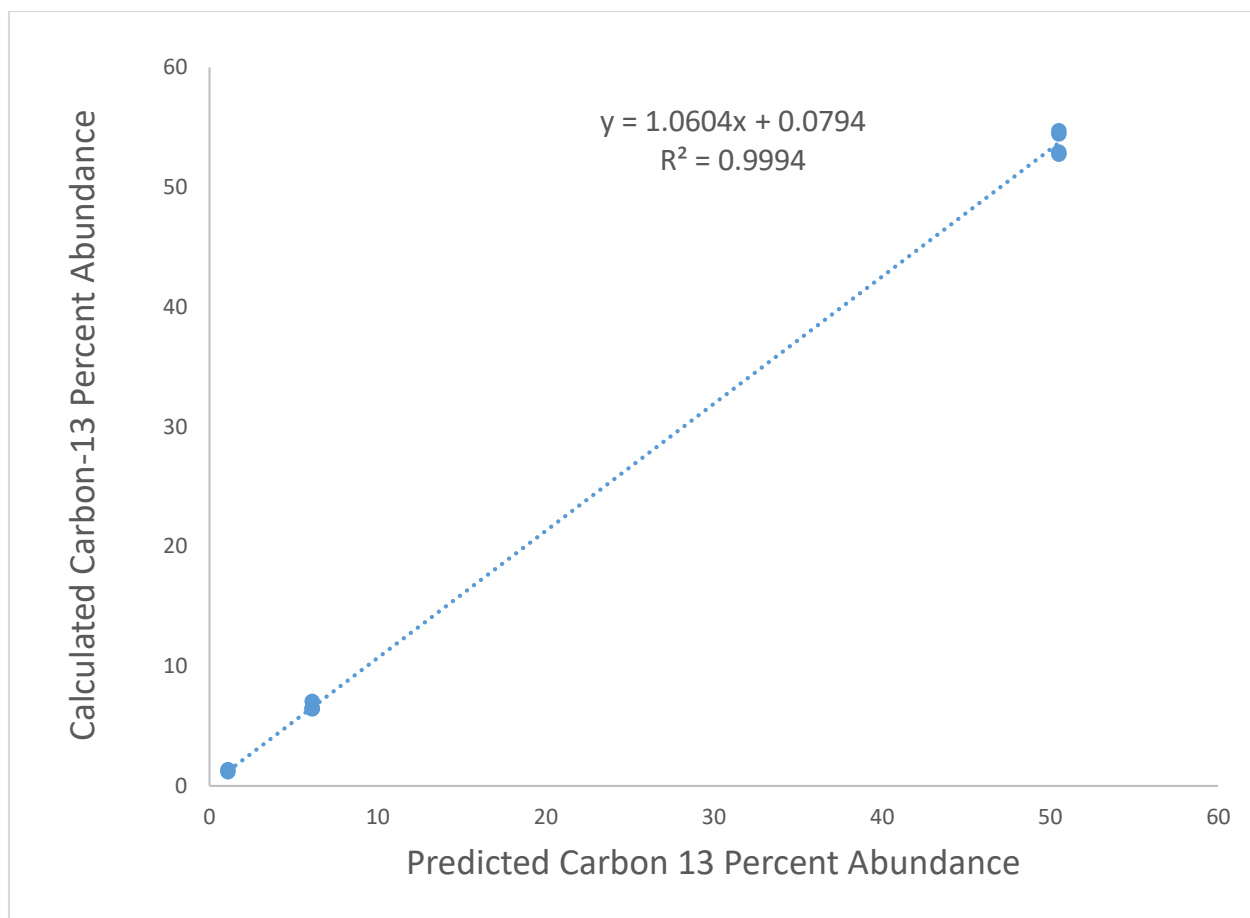


Figure 3.1 Gas Chromatography / Mass Spectrometry Calibration for Carbon-13 Detection

The x-axis represent the percentage of each compound labeled with ^{13}C and the y-axis represent the percentage of each compound labeled with ^{13}C detected by gas chromatography and mass spectrometry.

Calibration curves like these were created for various compounds of interest with the goal of confirming that the methods utilized to detect Carbon 13 in these compounds would be effective and precise. An interesting point about Figure 3.1 is that the point corresponding to the 100% naturally labeled sample does not read 0% ^{13}C detection. This is because carbon found in nature is known to have small amounts of carbon-13. With this confidence in the techniques in mind,

the experimental agenda was then turned towards working with the bovine embryos. As mentioned before, medium spiked with labeled carbohydrates was used to incubate these embryos. After successful incubation the medium is taken for analysis of the byproducts of the embryo metabolism. Each medium used by the bovine embryo initially was provided with the same concentration of uniformly ^{13}C labeled glucose and naturally labeled glucose. The labeling pattern ratio was chosen to maximize information gained from the experiment as glucose that did contain any labeling would not produce any ^{13}C labeled products, while glucose that was provided with 100 % ^{13}C labeling would cause the biological system to be saturated with ^{13}C creating products fully labeled with ^{13}C leading to hard calculations of metabolic pathway utilization. The fully labeled glucose creates this problem when the fully labeled substrate is the only carbon source. Since the embryo works with multiple substrates, this over saturation is not a problem. The labeled culture medium was provided to the bovine embryo and given a total of 6 hours for incubation. Shorter incubation times were not chosen because this was not enough time for the bovine embryo to incorporate significant amounts of substrate and convert them into analyzable products. Longer incubation times were not chosen because the embryo becomes unstable at these longer times leading to a shifted metabolism. After incubation, one product that was detected in the spent medium that was not provided in the fresh medium was lactic acid. This lactic acid was proven to have originated from the glucose provided in the medium because the lactic acid had statistically significant amounts of ^{13}C (Figure 3.2).

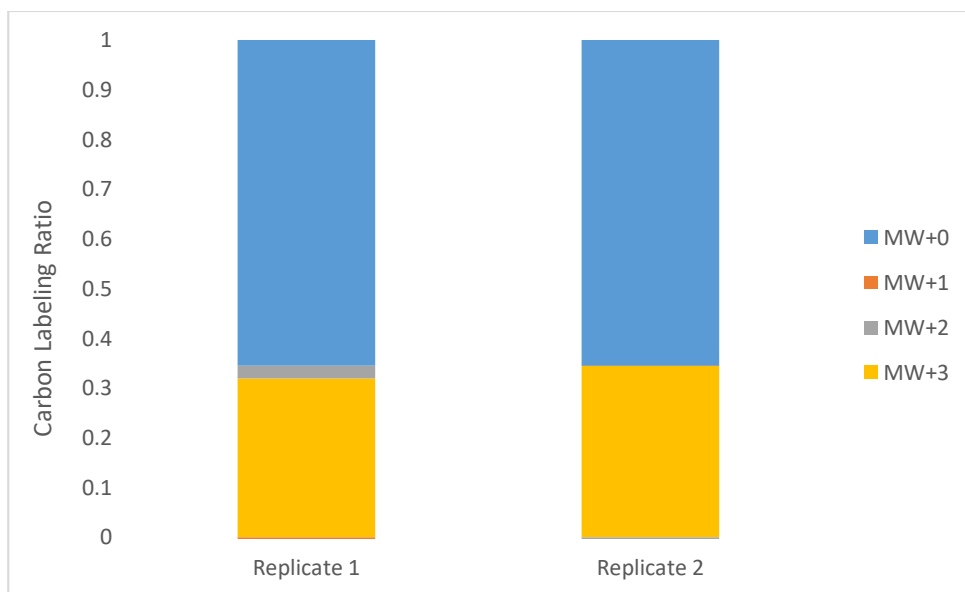


Figure 3.2 Isotopic Profile of Lactic Acid [123] Detected in Glucose Spent Medium

Each bar graph represents an individual injection of the glucose spent medium into the gas chromatogram mass spectrometer, [123] represents that the ions of interest contains 3 carbons and MW+3 represents the fraction of lactic acid that was detected by the mass spectrometer 3 Daltons above the normal molecular weight.

Unfortunately only 2 technical replicates could be extracted from the medium due to the low amount of sample that was produced for this method. As we can see the two technical replicates show a similar trend of the majority of lactic acid being detected at the original molecular weight and 3 Daltons above the original molecular weight. The appearance of the ions detected with higher molecular weight can be explained by the appearance of ^{13}C in the ions. As mentioned in Section 2.1, the lactic acid ions that enter the mass spectrometer are susceptible to fragmentation. One particular fragment that was detected with the mass spectrometer alongside

the three carbon ion shown in Figure 2.2 was a two carbon ion. This fragmented lactic acid ion also contained statistically significant amounts of ^{13}C (Figure 3.3).

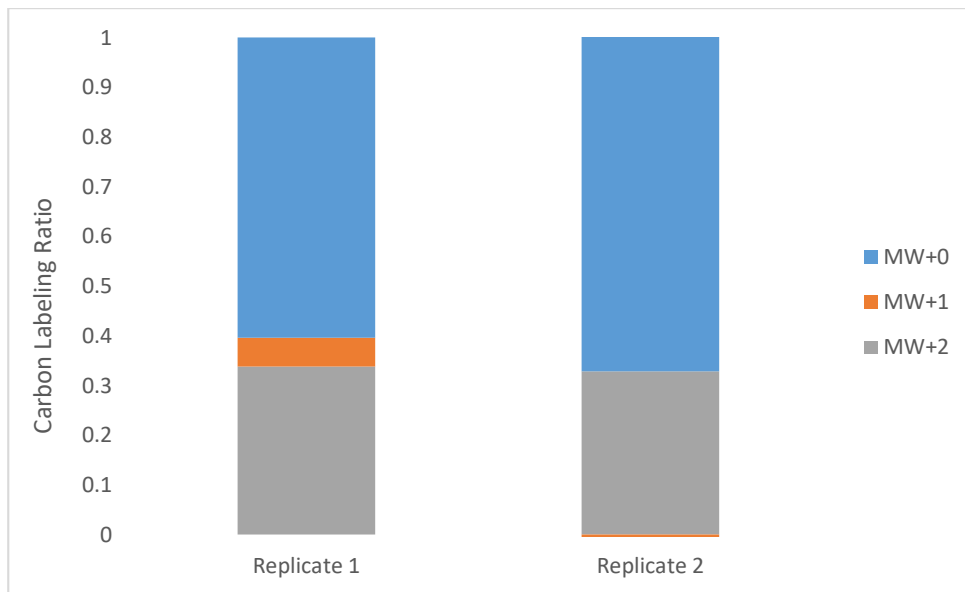


Figure 3.3 Isotopic Profile of Fragmented Lactic Acid [23] Detected in Glucose Spent Medium

Each bar graph represents an individual injection of the glucose spent medium into the gas chromatogram mass spectrometer, [23] represents that the ion of interest contains 2 carbons and MW+2 represents the fraction of lactic acid that was detected by the mass spectrometer to be 2 Daltons above the normal molecular weight.

This ion did not contain any ions with a molecular weight 3 Daltons above the original mass because there was only 2 carbons that are available for the ^{13}C labeling. Just like Figure 6.2, the majority of lactic acid ions were detected to be either unlabeled at the original molecular weight or labeled with ^{13}C at every available carbon. To confirm these results the same experiment was run again with another bovine embryo under the exact same conditions (Figure 3.4 and 3.5).

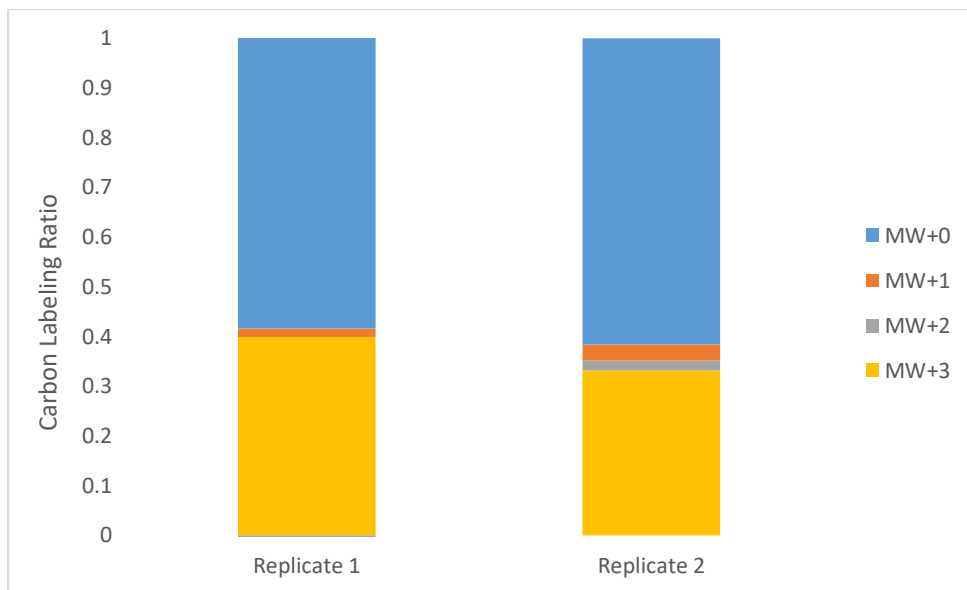


Figure 3.4 Second Embryo Isotopic Profile of Lactic Acid [123] Detected in Glucose Spent Medium

Each bar graph represents an individual injection of the glucose spent medium into the gas chromatogram mass spectrometer, [123] represents that the ion of interest contains 3 carbons and MW+2 represents the fraction of lactic acid that was detected by the mass spectrometer to be 2 Daltons above the normal molecular weight.

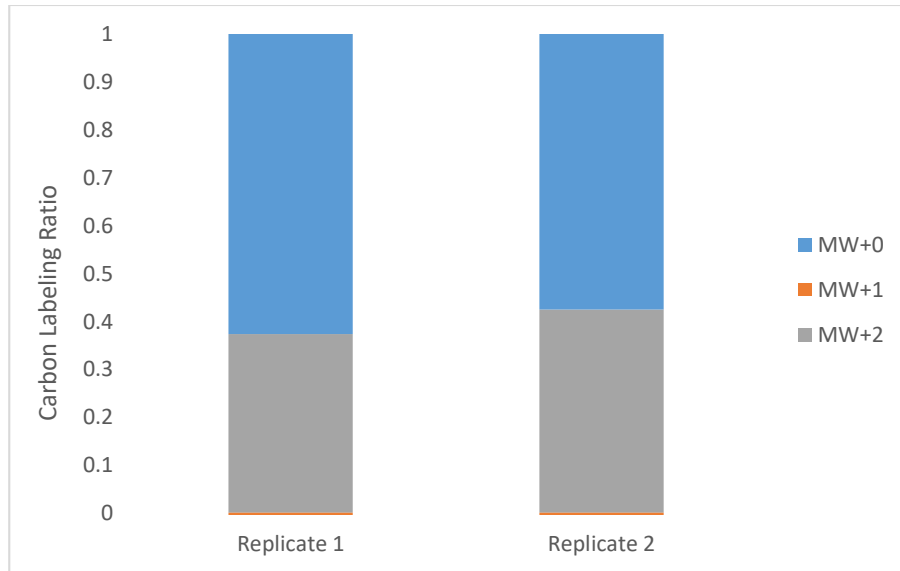


Figure 3.5 Second Embryo Isotopic Profile of Fragmented Lactic Acid [23] Detected in Glucose Spent Medium

Each bar graph represents an individual injection of the glucose spent medium into the gas chromatogram mass spectrometer, [23] represents that the ion of interest contains 2 carbons and MW+2 represents the fraction of lactic acid that was detected by the mass spectrometer to be 2 Daltons above the normal molecular weight.

As shown in Figures 3.4 and 3.5, the second embryo experiment produced similar isotopic profiles compared to the first experiment shown in Figures 3.2 and 3.3. This suggest that even though the embryos are different, the embryos used in the two experiments behave similarly. The biological and technical replicates results shown in Figure 3.2 through 3.5 were combined to give an average lactic acid isotopic profile for this particular experiment (Figure 3.6 and 3.7).

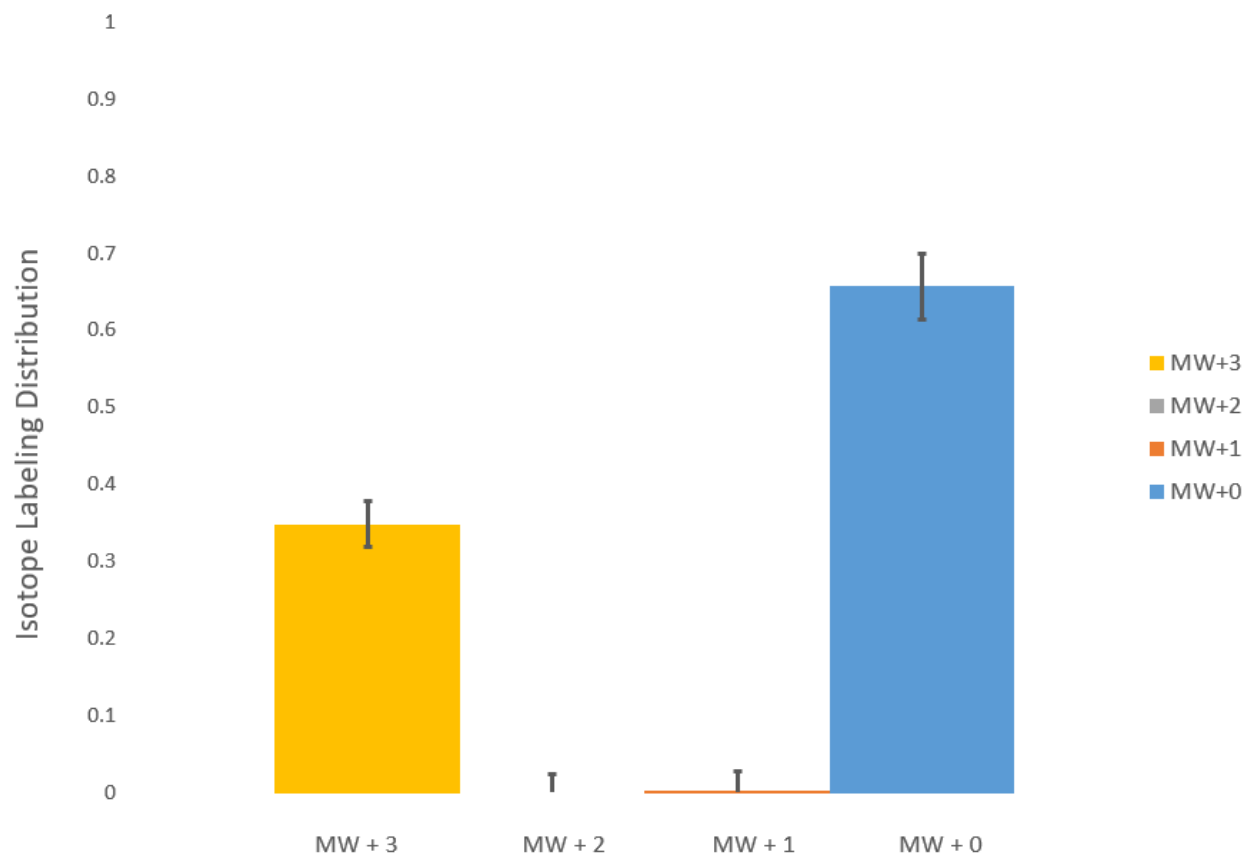


Figure 3.6 Average Isotopic Profile of Lactic Acid [123] Detected in Glucose Spent Medium

Each bar graph represents the molecular weight of lactic acid ions detected by the mass spectrometer, [123] represents that the ion of interest contains 3 carbons, MW+3 represents the fraction of lactic acid that was detected by the mass spectrometer to be 3 Daltons above the normal molecular weight and the error bars represent standard deviation of the biological and technical replicates shown in Figure 3.2 and 3.4.

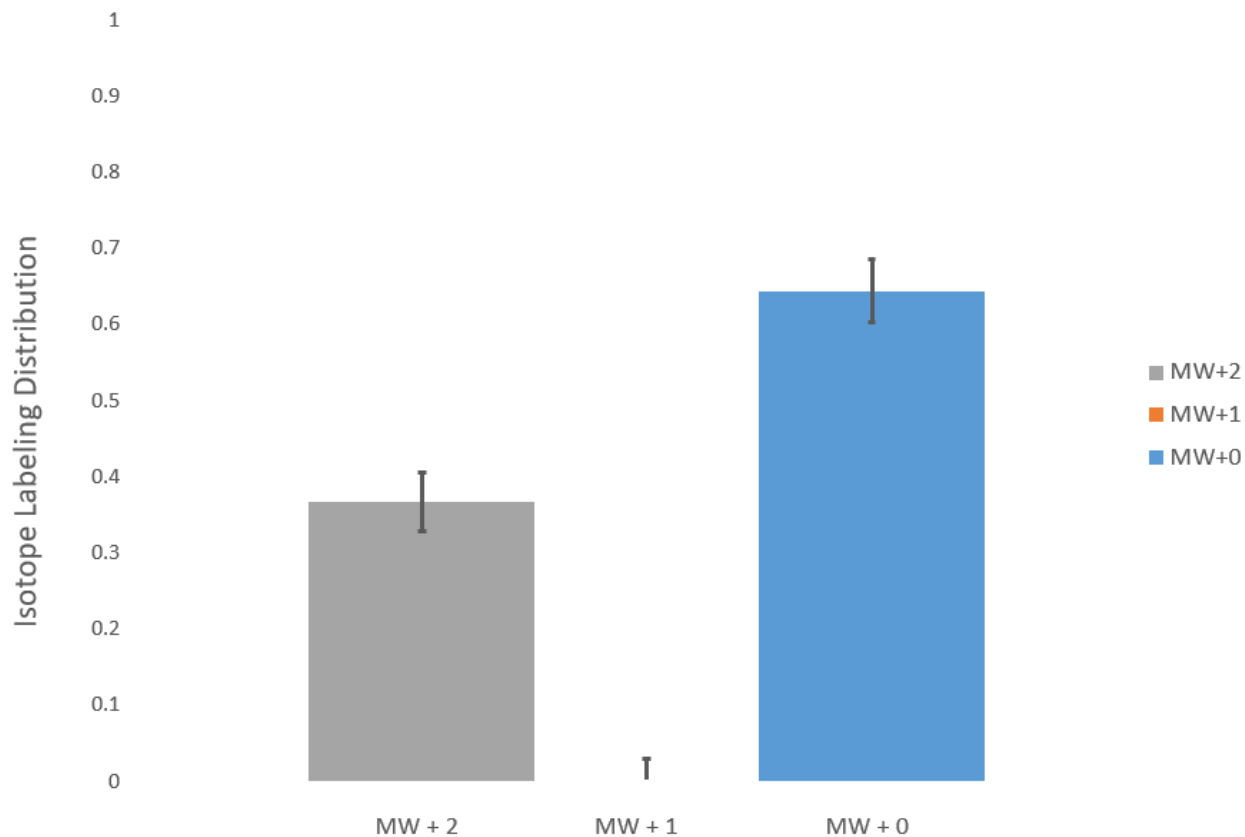


Figure 3.7 Average Isotopic Profile of Fragmented Lactic Acid [23] Detected in Glucose Spent Medium

Each bar graph represents the molecular weight of lactic acid ions detected by the mass spectrometer, [23] represents that the ion of interest contains 2 carbons, MW+2 represents the fraction of lactic acid that was detected by the mass spectrometer to be 2 Daltons above the normal molecular weight and the error bars represent standard deviation of the biological and technical replicates shown in Figure 3.3 and 3.5.

This is important for this set of experiments because if the monosaccharide being utilized for this pathway is labeled with ^{13}C at all 6 carbons then the resulting lactic acid formed would be labeled at all three positions. The significant amount of lactic acid detected that was labeled at all three carbons heavily suggests that those specific compounds were produced predominantly by aerobic glycolysis over other pathways that would result in a different labeling pattern. This phenomena heavily suggests that an effect called the Warburg effect is being utilized for the bovine embryo. This Warburg effect suggest that proliferating cells utilize the aerobic glycolysis pathway regardless of the availability of oxygen to facilitate the incorporation of nutrients into the biomass. Cells that don't follow the Warburg effect, like differentiated cells, would be heavily utilizing the oxidative phosphorylation pathway over aerobic glycolysis and thus would not create a significant amount of lactic acid (Vander 2009). The aerobic glycolysis is named aerobic even though it does not utilize oxygen because it is an alternative to the oxidative phosphorylation for biomass production. The next step in determining the utilization of this important pathway is to analyze under different conditions. One method to potentially shift the metabolism is to change the medium components that are fed to the embryos. The component that this experiment focuses on is the monosaccharide used in medium. The above experiment used glucose as the only simple sugar. Since it was mentioned earlier that glucose has been cited as a problematic substrate in medium, it was desired to change glucose into another sugar. This sugar used was fructose. Besides the change in simple sugar, all components of the experiment were kept constant including the other components in the medium. Just like the previous experiment, the concentration of the uniformly ^{13}C labeled was the same as the concentration of the naturally labeled monosaccharide. Another similarity between the experiments was that this

experiment also produced a spent medium that contained lactic acid. This is important because lactic acid was not an original component of the initial medium, thus it is confirmed to be a byproduct of the incubating embryo. The replicates of the fructose spent medium was collected and averaged to give an average lactic acid isotopic labeling profile (Figure 3.9).

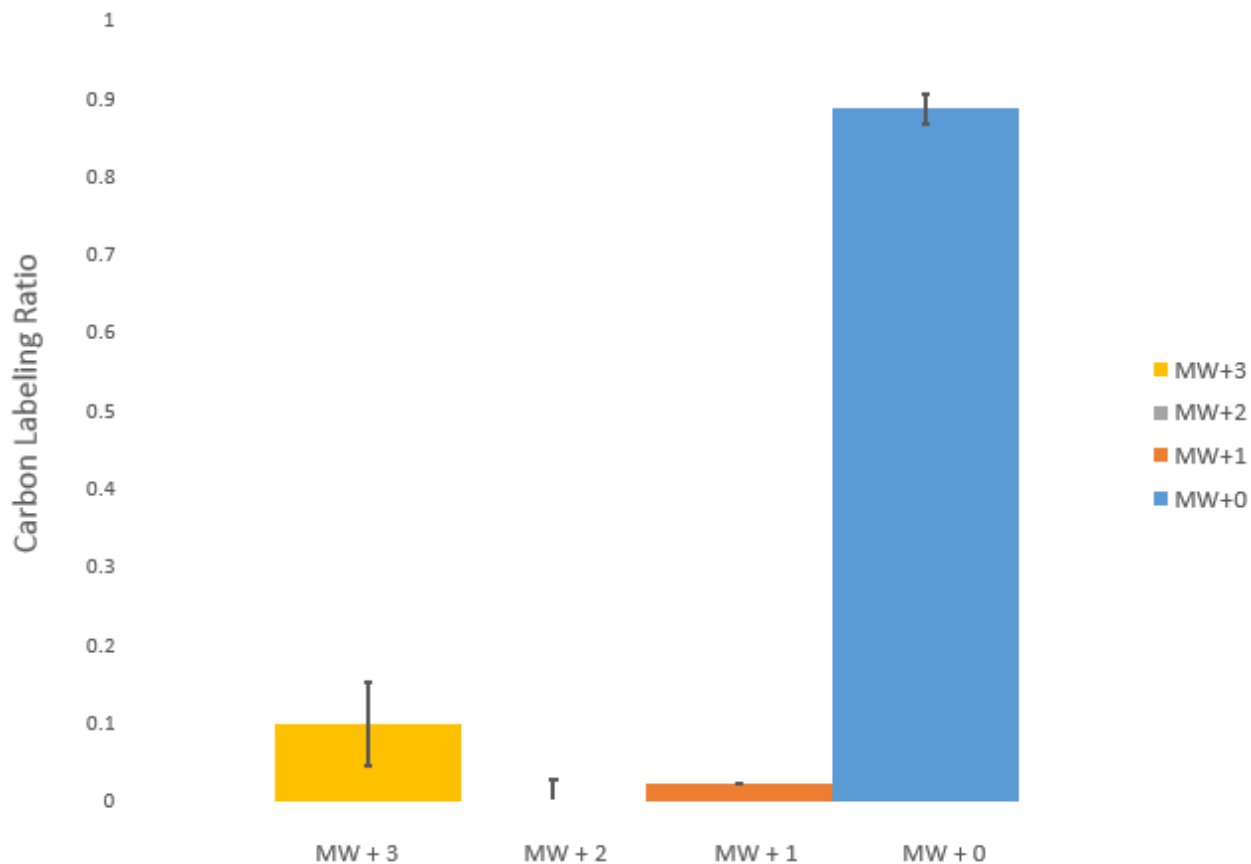


Figure 3.9 Average Isotopic Profile of Lactic Acid [123] Detected in Fructose Spent Medium

Each bar graph represents the molecular weight of lactic acid ions detected by the mass spectrometer, [123] represents that the ion of interest contains 3 carbons, MW+3 represents the fraction of lactic acid that was detected by the mass spectrometer to be 3 Daltons above the normal molecular weight and the error bars represent standard deviation of the replicates.

Just like the experiment with the bovine embryo in the glucose medium, the lactic acid was also detected with a fragmented 2 carbon lactic acid (Figure 30).

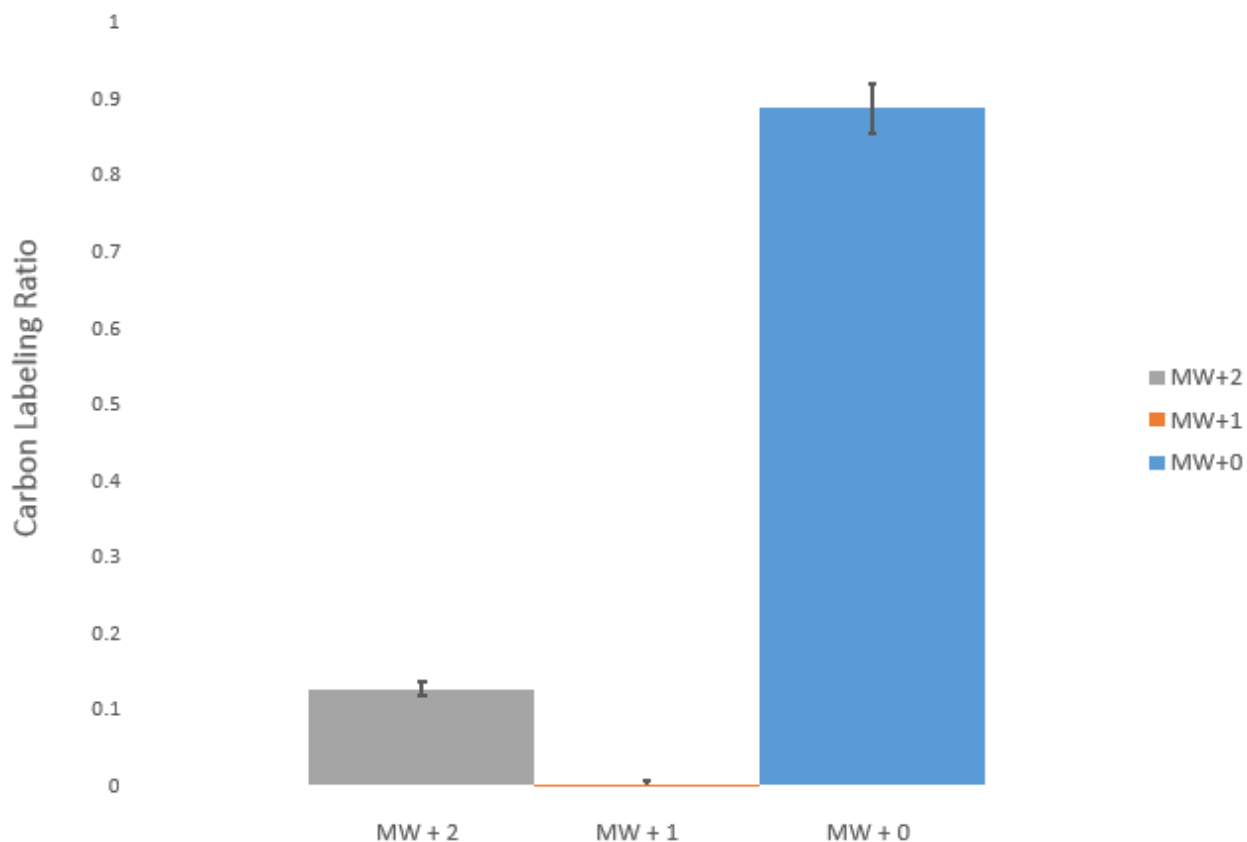


Figure 3.10 Average Isotopic Profile of Fragmented Lactic Acid [23] Detected in Fructose Spent Medium

Each bar graph represents the molecular weight of lactic acid ions detected by the mass spectrometer [23] represents that the ion of interest contains 2 carbons, MW+2 represents the fraction of lactic acid that was detected by the mass spectrometer to be 2 Daltons above the normal molecular weight and the error bars represent standard deviation of the replicates.

The isotopic profile shown in Figures 3.9 and 3.10 have a similar profile to the averaged glucose experiments shown in Figure 3.6 and 3.7. These profiles show that the most abundant labeled ion detected by the mass spectrometer was always the ion that was labeled with ^{13}C at all available carbons. This heavily suggest that aerobic glycolysis is also being utilized for an embryo incubating in fructose medium. The main difference between the averaged profiles created in the glucose and fructose medium was how abundant this ion was in relation to the unlabeled ion. The fully labeled ion was detected in around 30 to 40 percent of the lactic acid ions created in the glucose medium. On the other hand, fructose medium created only around 5 to 15 percent of the lactic acid ions detected. This difference will be evaluated in more depth in the next section.

3.2 Fluxomic Evaluation

A helpful analysis used to better understand an organism is a fluxomic analysis. This analysis looks to elucidate the metabolic pathway utilization by defining reaction rates taken place within the organism of interest. Although there are multiple approaches to a fluxomic evaluation, this paper focuses on metabolic flux analysis (covered in more detail in Sections 2.3 and 2.4) to accomplish this evaluation. The first step in setting up this analysis is to create a model that contains reaction rates that are known to be used in the organism of interest. The model used to represent the bovine embryo used reaction rates from the website HumanCyc to represent mammalian cells (HumanCyc 2017). The next step for a metabolic flux analysis is to run a labeling experiment to get an understanding on the usage of these reactions. The labeling experiment utilized focused on ^{13}C as the label and is described in more detail in the previous section. The important components of this labeling experiment are glucose, fructose and lactic acid because these components contained ^{13}C labeling. The labeling is important because

simulating reaction rates will be used to try and understand the labeling patterns observed under the different conditions. Using a program mentioned in more detail in Section 2.4, a global optimization is used to change reaction rates until an optimized reaction rate for each reaction is determined. The optimal reaction rates will most closely simulate the isotopomer profiles shown in Figures 3.6, 3.7, 3.9 and 3.10 depending on the experimental condition that is being analyzed. The comparison of the simulated isotopomer distributions from a glucose medium to the experimental distributions described in Figures 3.6 and 3.7 showed a similar trend (Figure 3.11 and Figure 3.12).

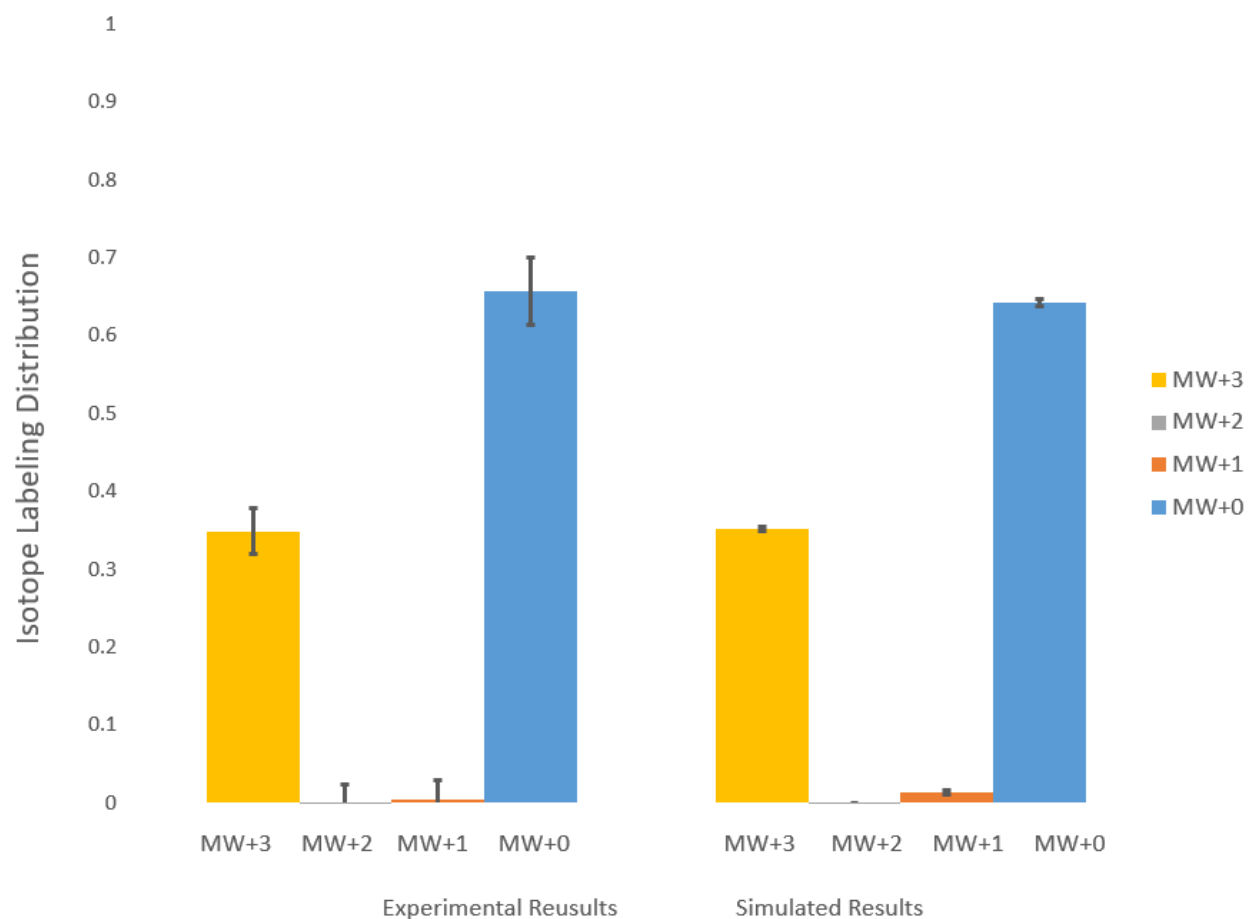


Figure 3.11 Comparing Experiment and Simulated Isotopic Profiles for Lactic Acid [123] in Glucose Spent Medium

Each bar graph represents the molecular weight of lactic acid ions, [123] represents that the ion of interest contains 3 carbons and MW+3 represents the fraction of lactic acid that was detected by the mass spectrometer to be 3 Daltons above the normal molecular weight. The experimental results correspond to Figure 3.6 and the simulated results are the average of 100 optimized isotopic labeling profiles created from the metabolic flux analysis.

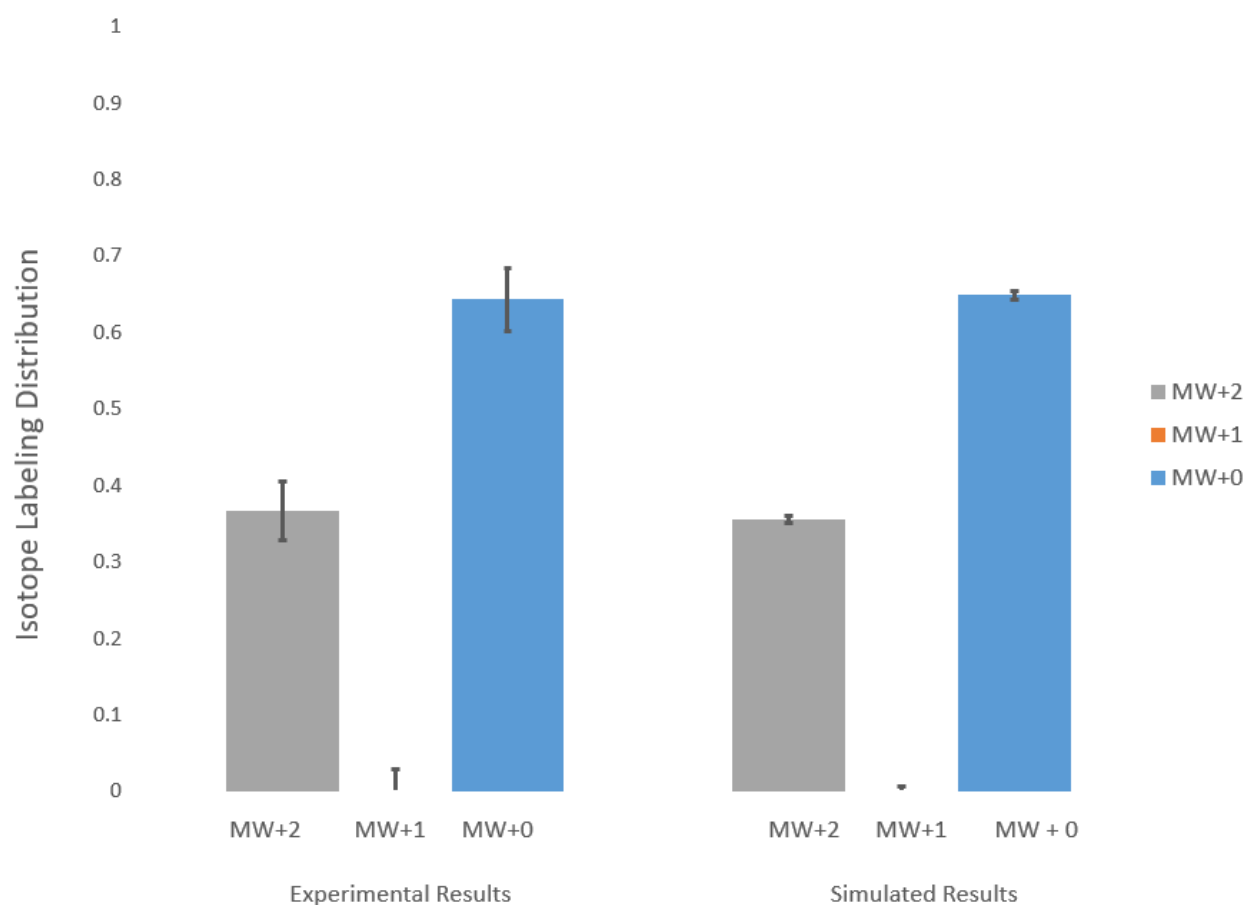


Figure 3.12 Comparing Experiment and Simulated Isotopic Profiles for Fragmented Lactic Acid [23] in Glucose Spent Medium

Each bar graph represents the molecular weight of fragmented lactic acid ions, [23] represents that the ion of interest contains 2 carbons and MW+2 represents the fraction of lactic acid that was detected by the mass spectrometer to be 2 Daltons above the normal molecular weight. The experimental results correspond to Figure 3.7 and the simulated results are the average of 100 optimized isotopic labeling profiles created from the metabolic flux analysis.

The model created reaction rates that simulate lactic acid labeling patterns that closely compare to the actual labeling pattern for both ions detected in the glucose spent culture medium. The same comparison of labeling patterns was observed for the fructose spent medium from the experimental conditions shown in Figure 3.9 and 3.10 with the simulated results (Figure 3.13 and 3.14).

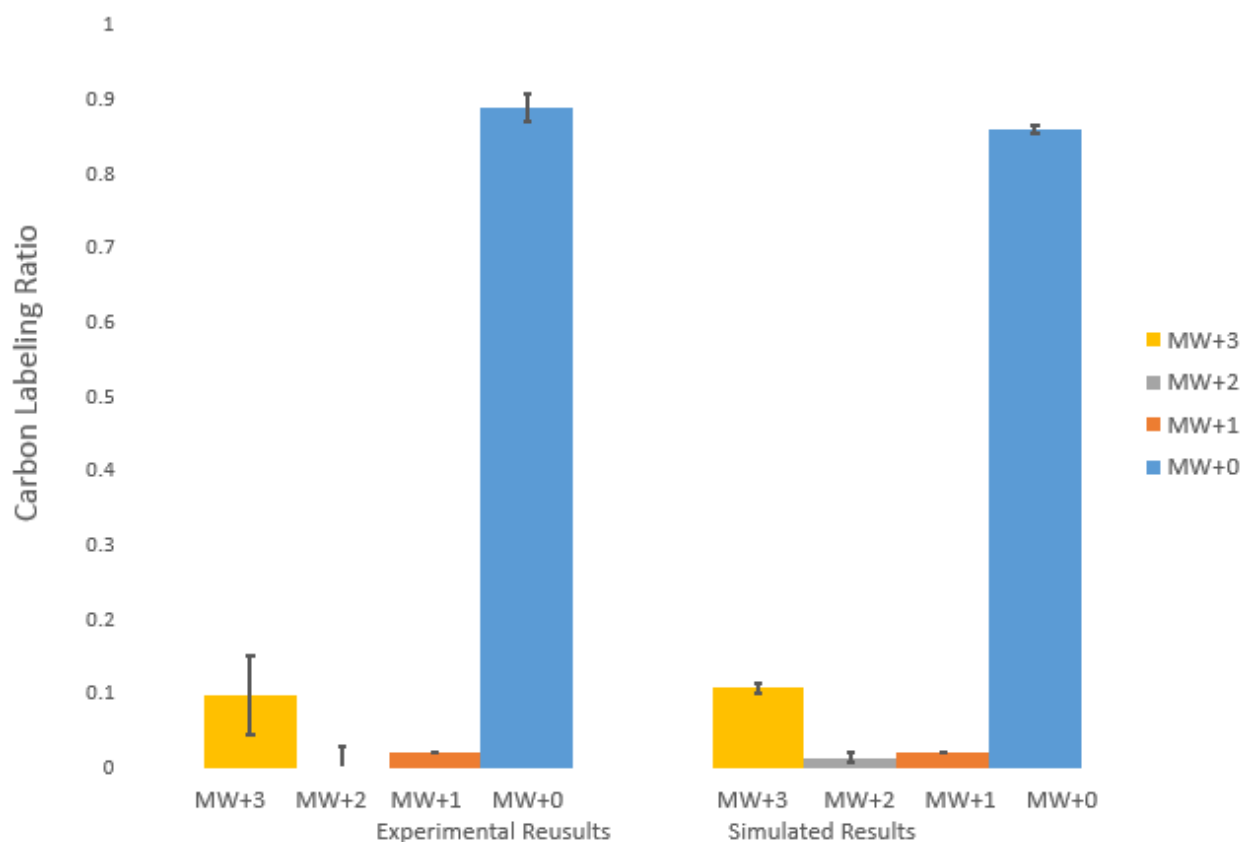


Figure 3.13 Comparing Experiment and Simulated Isotopic Profiles for Lactic Acid [123] in Fructose Spent Medium

Each bar graph represents the molecular weight of lactic acid ions, [123] represents that the ion of interest contains 3 carbons and MW+3 represents the fraction of lactic acid that was detected by the mass spectrometer to be 3 Daltons above the normal molecular weight. The experimental results correspond to Figure 3.9 and the simulated results are the average of 100 optimized isotopic labeling profiles created from the metabolic flux analysis.

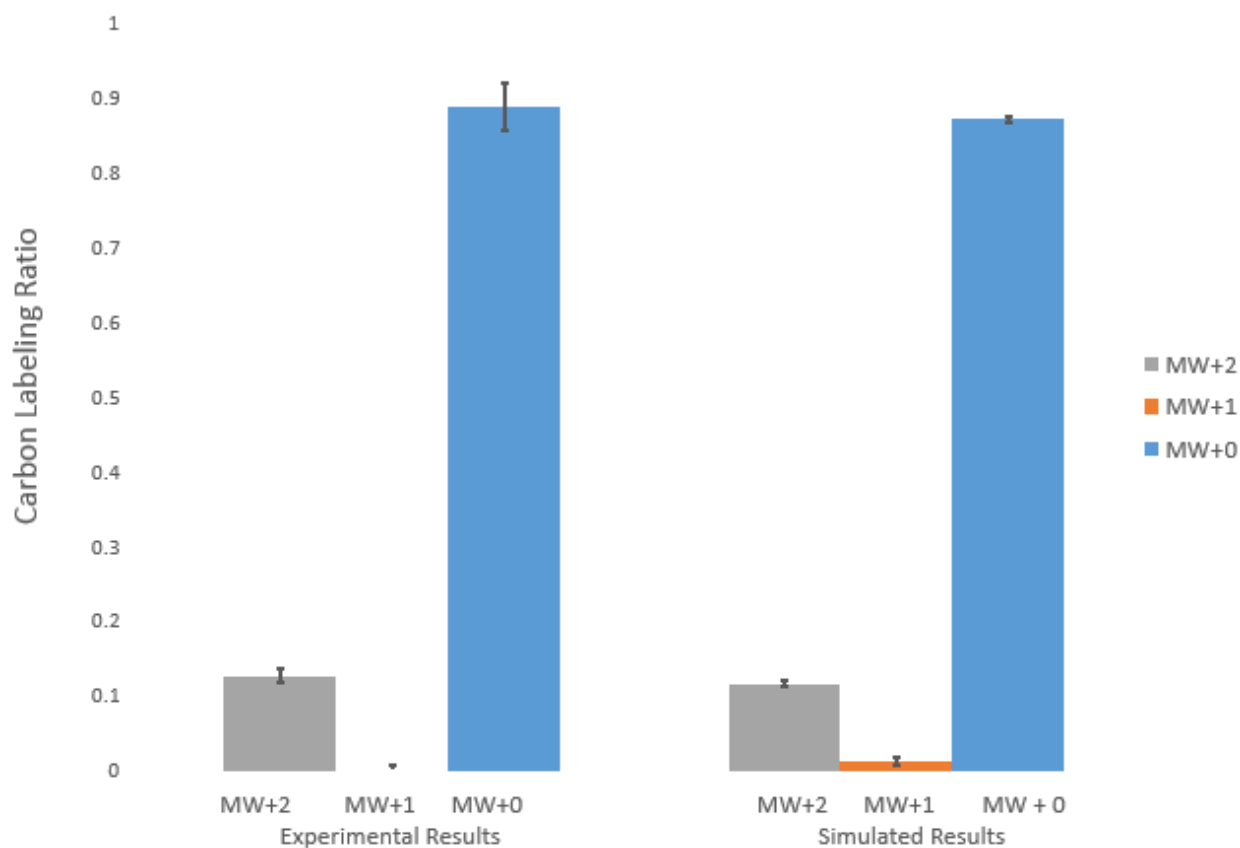


Figure 3.14 Comparing Experiment and Simulated Isotopic Profiles for Fragmented Lactic Acid [23] in Fructose Spent Medium

Each bar graph represents the molecular weight of fragmented lactic acid ions, [23] represents that the ion of interest contains 2 carbons and MW+2 represents the fraction of lactic acid that was detected by the mass spectrometer to be 2 Daltons above the normal molecular weight. The experimental results correspond to Figure 3.7 and the simulated results are the average of 100 optimized isotopic labeling profiles created from the metabolic flux analysis.

The simulated profiles shown in Figures 3.12 and 3.13 were created using the average of 100 optimized models for each condition. Each model was defined using the same reactions that were

acquired by using HumanCyc (HumanCyc 2017). The model included reactions that were important for the carbon metabolism of the compounds that showed ^{13}C labeling. The averaged results of these models with the values and standard deviations of these reaction rates were combined for each culture medium condition (Figure 3.15 and 3.16).

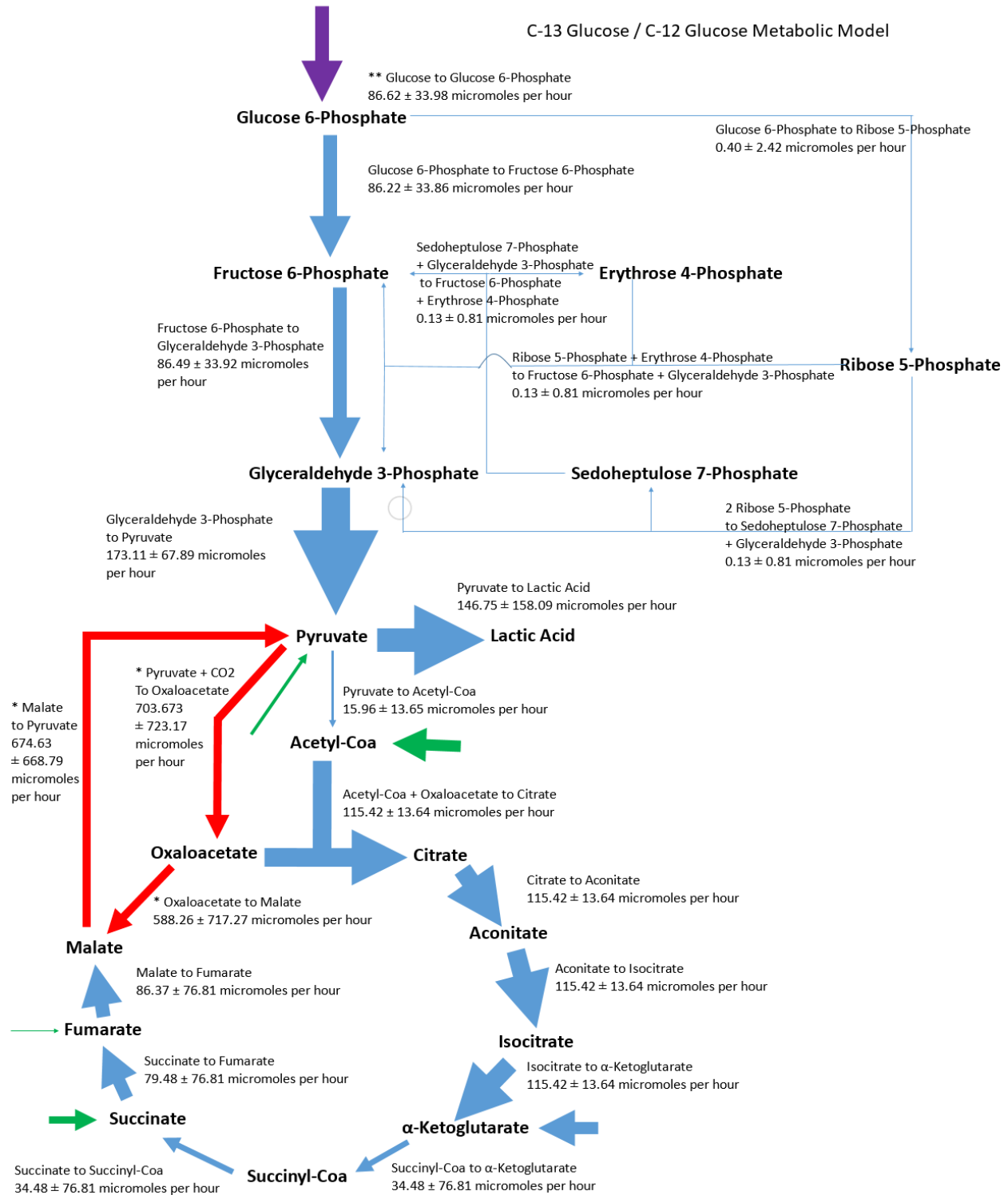


Figure 3.15 Metabolic Model of Bovine Embryo in Glucose Medium

The bolded words represent important metabolites in the bovine embryo, the arrows represent potentially multiple reactions conglomerated progressing from the substrate to the product and the size of the arrows represent the relative reaction rates of the averaged optimized model. Specific arrows to mention include the red arrows labeled with a single star represent unscalable reactions with high standard deviations, the purple arrows with two stars represent the transport reactions of the 50 percent labeled substrate and the green arrows unlabeled represent sources of unlabeled carbon.

C-13 Fructose / C-12 Fructose Metabolic Model

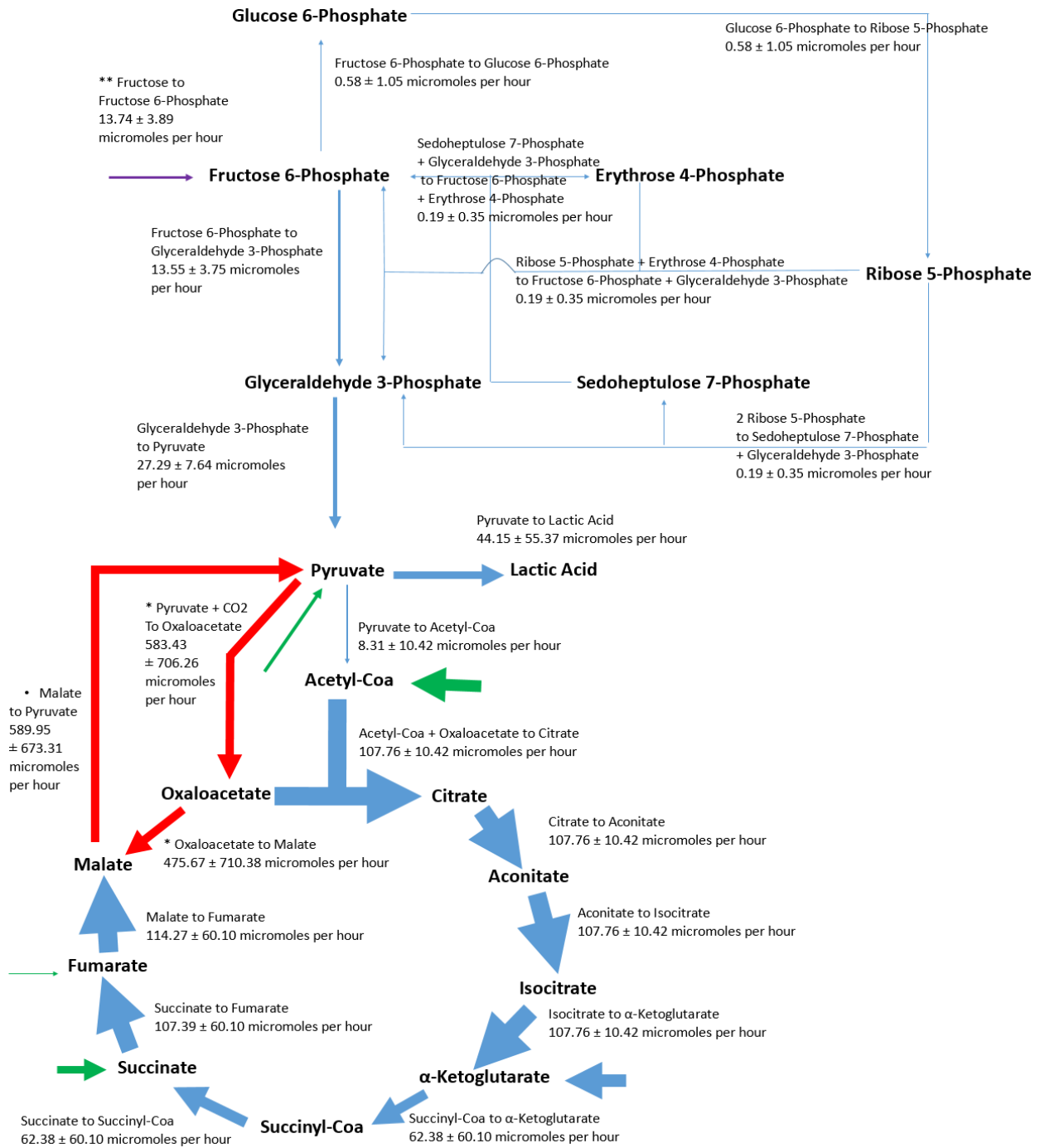


Figure 3.16 Metabolic Model of Bovine Embryo in Fructose Medium

The bolded words represent important metabolites in the bovine embryo, the arrows represent potentially multiple reactions conglomerated progressing from the substrate to the product and the size of the arrows represent the relative reaction rates of the averaged optimized model. Specific arrows to mention include the red arrows labeled with a single star represent unscalable reactions with high standard deviations, the purple arrows with two stars represent the transport reactions of the 50 percent labeled substrate and the green arrows unlabeled represent sources of unlabeled carbon.

Since the experiment only detected one product with ^{13}C labeling (lactic acid) not all of the reaction rates of the model were restricted to a specific value. The presence of other products with labeling, like TCA derived amino acids, would allow the red reactions to have a lower standard deviation. The location of the purple arrow is different for each model because it depends on the substrate that is fed to the bovine embryo. The glucose model has the 50% labeled substrate transported into the embryo and converted to glucose 6-phosphate, while the fructose model has the 50% labeled substrate transported into the embryo and converted to fructose 6-phosphate. Although the substrate feeds into different locations of the model, both carbohydrates are used to fuel the important glycolysis pathway. The main difference between these models is shown by the utilization of this pathway. The Figure 3.16 fructose model shows a dramatic decrease of the glycolytic reaction rates compared to the Figure 3.15 glucose model. One of these reaction utilizes an important enzyme mentioned earlier. The enzyme is glyceraldehyde 3 phosphate-dehydrogenase and is used to convert glyceraldehyde 3-phosphate into pyruvate. This enzyme is important because it is shown in other organisms to bind to a messenger RNA that creates the important cell signaling compound called interferon gamma

(Nicholls 2012). Other studies have shown that glycolysis is intimately connected with the control of interferon secretion and signaling in other cell types (Chang 2013). This heavily suggests that when there is a shift in the flux for glycolytic reaction rates, important cell signaling interferon compounds are released at different rates. The difference in the reaction rate between Figure 3.15 and Figure 3.16 heavily suggests that glucose medium will lead to a difference in the amount of interferon secretion and signaling compared to the fructose medium. To confirm the difference between the reaction rates of the two different models it is helpful to view the distribution of the optimized reaction rates that lead to the averages shown in Figure 3.15 and 3.16. A sensitivity analysis for the consolidated reaction converting glyceraldehyde 3-phosphate to pyruvate was created to illustrate the difference (Figure 3.17).

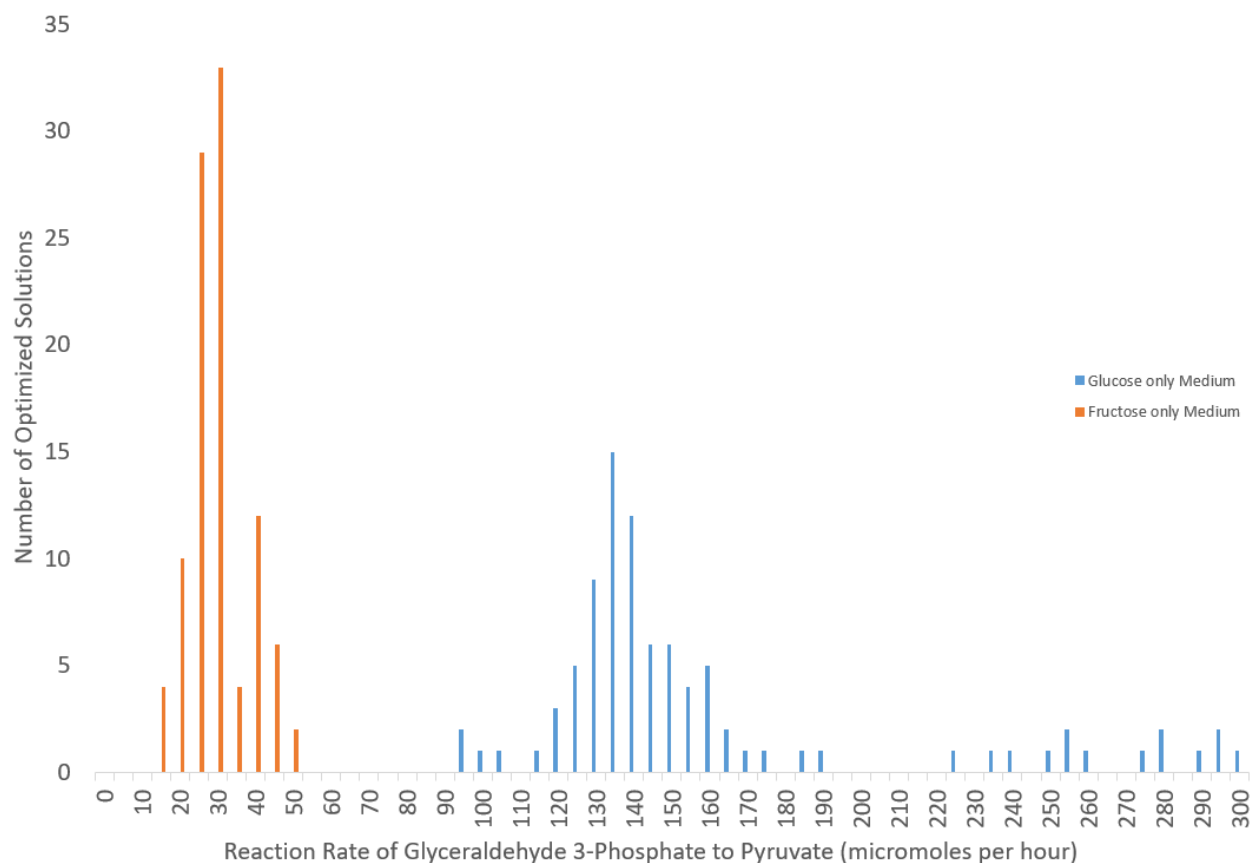


Figure 3.17 Sensitivity Analysis of Glyceraldehyde 3-Phosphate to Pyruvate Reaction

Each bar graph represents the number of optimized reaction rates within 5 micromoles per hour, the orange bars represent reactions optimized for a model based on a fructose medium and the blue bars represent reactions optimized for a model based on a glucose medium.

The distribution of the reaction rates confirms that the embryo in the glucose medium utilizes the aerobic glycolysis pathway reaction to a greater extent than the embryo in the fructose medium.

This suggests that by changing the carbohydrates provided, the utilization of the aerobic glycolysis pathway can be controlled.

Chapter 4: Conclusions

This study focused on better understanding the bovine embryo in the blastocyst stage so that some of the problems of embryo production could be alleviated. This was accomplished using a fluxomic analysis that took advantage of ^{13}C labeling. This project was the first of its kind to utilize ^{13}C labeling for a fluxomic evaluation of the bovine embryo to evaluate substrate utilization. The ^{13}C was provided as a simple sugar that was converted into products by the bovine embryo. The detection of lactic acid in the medium after incubation heavily suggests that the bovine embryo produces lactic acid during embryo production. By detecting the ^{13}C labeling in the newly formed lactic acid, the study was able to confirm the utilization of the aerobic glycolysis pathway. This pathway has been shown to be important in pregnancies for many biological activities including the use of certain enzymes to control cell signaling interferon molecules. The utilization of this pathway was also detected to be more abundant when glucose was the only sugar provided compared to fructose. These results were confirmed using a metabolic model that highlights the differences of relative reaction rates. Future studies could be used to determine the utilization of the aerobic glycolysis pathway for in vivo embryos. Using this knowledge, the relative amounts of fructose and glucose can be used to tune the embryo to behave similarly to its' in vivo counterpart. This tuning process could also be used to control the abundance of cell signaling molecules important for pregnancy.

Chapter 5: Experimental Procedures

5.1 Bovine Embryo Cell Growth

The bovine embryo was acquired from the company Applied Reproductive Technology. Each biological replicate was pooled with 5 total embryos and put in a synthetic oviduct fluid (Supplementary Figure 1). The embryos were provided with 40 uL of the media and prepared on 30 mm dish covered with mineral. Prepared dishes were incubated in 5 % CO₂ and 5 % O₂ at 38.5 °C for 6 hours. Medium spent by blastocysts was collected and stored in – 80 °C for analysis.

5.2 Isotope Labeling Experiment

¹³C labeled glucose and fructose was acquired from the company Cambridge Isotope Laboratories. The labeled carbohydrates were provided to the culture medium at a total sugar concentration of 1.5 mM along with other compounds to simulate embryo production (Supplementary Figure 1). After bovine embryo incubation the spent medium was taken for gas chromatography mass spectrometry analysis. The spent medium was then taken and lyophilized using a MicroModulyo 1.5L Freeze Dryer from Thermo Scientific for two days. The anhydrous medium was taken from the freeze dryer and prepared for derivatization. To prepare for the derivatization, 40 uL of N-methyl-N-tert-butyl-dimethyl-silyl trifluoroacetamide and 20 uL of 20 mg/mL of methionine hydrochloride in dimethylformamide was added to the anhydrous medium. The newly formed solution was then transferred into Thermo Scientific 11mm Clear Glass Crimp/ Snap Top Vials. The vials were then heated at 70 degrees Celsius for about 1.5 hours.

The newly derivatized medium was then immediately put into the autosampler for gas chromatography mass spectrometry analysis. Each technical replicate involved taking 5 μ L injections of the solution with a 2 split ratio.

5.3 Fluxomic Evaluation from Isotopomer Data

This experiment employed a ^{13}C metabolic flux analysis program called NMR2Flux+ for evaluation of metabolic fluxes from isotopomer data (Sriram 2007). The program is supplied with information on the metabolic network including metabolite names, chemical reaction stoichiometries, carbon atom rearrangement, isotopically labeled forms of the carbon source, mass isotopomer measurements and relationship of the measured mass isotopomer fragments to central carbon precursors. It uses a flux-isotopomer model, nonlinear optimization and Monte Carlo statistical analysis to calculate fluxes and confidence intervals from a given set of amino acid mass isotopomer measurements. To assess how well the evaluated fluxes account for the supplied isotopomer measurements, the program uses a sum of squared residuals.

Supplementary Information

Component	Molarity in Medium (mM)
CaCl ₂ • 2H ₂ O	1.17
GlutaMAX	1
Glycine	0.1
KH ₂ • PO ₄	1.19
KCl	7.16
L-Alanine	0.1
L-Arginine•HCl	0.1
L-Asparagine	0.1
L-Aspartic Acid	0.1
L-Cystine	0.1
L-Glutamic Acid	0.1
L-Histidine	0.05
L-Isoleucine	0.2
L-Leucine	0.2
L-Lysine•HCl	0.2
L-Methionine	0.05
L-Phenylalanine	0.1
L-Proline	0.1
L-Serine	0.1
L-Threonine	0.2
L-Tryptophan	0.02
L-Tyrosine	0.1
L-Valine	0.2
MgCl ₂ • 6H ₂ O	0.49
NaCl	107.7
NaHCO ₃ •	25.07

Supplementary Figure 1: Molarity of Compounds in Medium Provided

Concentrations of the various compounds provided to the bovine embryo for both the glucose and fructose medium.

List of Figures

Figure 2.1 Example of a Gas Chromatogram

Figure 2.2 Example of a Mass Spectrum

Figure 2.3 Silylation Derivatization Reaction for Gas Chromatography Utilization

Figure 2.4 Methoximation Reaction

Figure 2.5 Comparing Experimental and Theoretical Mass Spectrums

Figure 2.6 Example of a Gas Chromatogram with Labeled Peaks

Figure 2.7 Sample Metabolic Network

Figure 2.8 Sample Matrix for Compound Balancing

Figure 2.9 Separated Sample Matrix for Compound Balancing

Figure 2.10 Calculating Dependent Reaction Rates

Figure 2.11 Sample Metabolic Network with Labeling Patterns

Figure 2.12 Cumomers System for a Three Atom Compound

Figure 2.13 Determining Labeling Pattern from Cumomer Ratios for a Three Atom Compound

Figure 2.14 Example of Cumomer Balances Arranged By Cumomer Order

Figure 2.15 Example of Blank First Order Cumomer Matrix Arranged

Figure 2.16 Example of Generation Matrix for First Order Cumomers

Figure 2.17 Example of Consumption Matrix for First Order Cumomers

Figure 2.18 Example of First Order Cumomer Balance in Matrix Form

Figure 2.19 Example of Second Order Cumomer Balance in Matrix Form

Figure 2.20 Example of Third Order Cumomer Balance in Matrix Form

Figure 3.1 Gas Chromatography / Mass Spectrometry Calibration for Carbon-13 Detection

Figure 3.2 Isotopic Profile of Lactic Acid [123] Detected in Glucose Spent Medium

Figure 3.3 Isotopic Profile of Fragmented Lactic Acid [23] Detected in Glucose Spent Medium

Figure 3.4 Second Embryo Isotopic Profile of Lactic Acid [123] Detected in Glucose Spent Medium

Figure 3.5 Second Embryo Isotopic Profile of Fragmented Lactic Acid [23] Detected in Glucose Spent Medium

Figure 3.6 Average Isotopic Profile of Lactic Acid [123] Detected in Glucose Spent Medium

Figure 3.7 Average Isotopic Profile of Fragmented Lactic Acid [23] Detected in Glucose Spent Medium

Figure 3.8 Aerobic Glycolysis Carbon Rearrangement

Figure 3.9 Average Isotopic Profile of Lactic Acid [123] Detected in Fructose Spent Medium

Figure 3.10 Average Isotopic Profile of Fragmented Lactic Acid [23] Detected in Fructose Spent Medium

Figure 3.11 Comparing Experiment and Simulated Isotopic Profiles for Lactic Acid [123] in Glucose Spent Medium

Figure 3.12 Comparing Experiment and Simulated Isotopic Profiles for Fragmented Lactic Acid [23] in Glucose Spent Medium

Figure 3.13 Comparing Experiment and Simulated Isotopic Profiles for Lactic Acid [123] in Fructose Spent Medium

Figure 3.14 Comparing Experiment and Simulated Isotopic Profiles for Fragmented Lactic Acid [23] in Fructose Spent Medium

Figure 3.15 Metabolic Model of Bovine Embryo in Glucose Medium

Figure 3.16 Metabolic Model of Bovine Embryo in Fructose Medium

Figure 3.17 Sensitivity Analysis of Glyceraldehyde 3-Phosphate to Pyruvate Reaction

Supplementary Figure 1: Molarity of Compounds in Medium Provided

Bibliography

1. Perkel, Kayla J., et al. “The ART of Selecting the Best Embryo: A Review of Early Embryonic Mortality and Bovine Embryo Viability Assessment Methods.” *Molecular Reproduction and Development*, vol. 82, no. 11, Nov. 2015, pp. 822–838. *Wiley Online Library*, doi:10.1002/mrd.22525.
2. Lonergan, P., and T. Fair. “In Vitro-Produced Bovine embryos—Dealing with the Warts.” *Theriogenology*, vol. 69, no. 1, Jan. 2008, pp. 17–22. *ScienceDirect*, doi:10.1016/j.theriogenology.2007.09.007.
3. Singh, R., and K. D. Sinclair. “Metabolomics: Approaches to Assessing Oocyte and Embryo Quality.” *Theriogenology*, vol. 68, no. Supplement 1, Sept. 2007, pp. S56–S62. *ScienceDirect*, doi:10.1016/j.theriogenology.2007.04.007.
4. European Society of Human Reproduction and Embryology. “In vitro maturation: Do eggs matured in the laboratory result in babies with large offspring syndrome?” *ScienceDaily*. *ScienceDaily*, 30 June 2010. <www.sciencedaily.com/releases/2010/06/100630071148.htm>
5. Chen, Zhiyuan et al. “Large Offspring Syndrome.” *Epigenetics* 8.6 (2013): 591–601.
6. *Prenatal Development | Definition and Patient Education*. 1 Dec. 2013, <https://web.archive.org/web/20131201081856/http://www.healthline.com/galecontent/prenatal-development>.
7. Chang, Chih-Hao, et al. “Posttranscriptional Control of T Cell Effector Function by Aerobic Glycolysis.” *Cell*, vol. 153, no. 6, June 2013, pp. 1239–1251. *ScienceDirect*, doi:10.1016/j.cell.2013.05.016.

8. Mazurek, Sybille. "Pyruvate Kinase Type M2: A Key Regulator of the Metabolic Budget System in Tumor Cells." *The International Journal of Biochemistry & Cell Biology*, vol. 43, no. 7, July 2011, pp. 969–980. *ScienceDirect*, doi:10.1016/j.biocel.2010.02.005.
9. Nicholls, Craig, et al. "GAPDH: A Common Enzyme with Uncommon Functions." *Clinical and Experimental Pharmacology and Physiology*, vol. 39, no. 8, Aug. 2012, pp. 674–679. *Wiley Online Library*, doi:10.1111/j.1440-1681.2011.05599.x.
10. Ashkar, Ali A., et al. "Interferon γ Contributes to Initiation of Uterine Vascular Modification, Decidual Integrity, and Uterine Natural Killer Cell Maturation during Normal Murine Pregnancy." *The Journal of Experimental Medicine*, vol. 192, no. 2, July 2000, pp. 259–270.
11. Leese, H. J., et al. "Embryo Viability and Metabolism: Obeying the Quiet Rules." *Human Reproduction*, vol. 22, no. 12, pp. 3047–3050.
12. Bermejo-Alvarez, P., et al. "Effect of Glucose Concentration during in Vitro Culture of Mouse Embryos on Development to Blastocyst, Success of Embryo Transfer, and Litter Sex Ratio." *Molecular Reproduction and Development*, vol. 79, no. 5, May 2012, pp. 329–336. *Wiley Online Library*, doi:10.1002/mrd.22028.
13. Kimura, Koji, et al. "Sexual Dimorphism in Interferon- τ Production by In Vivo-Derived Bovine Embryos." *Molecular Reproduction and Development*, vol. 67, Feb. 2004, pp. 193–9. *ResearchGate*, doi:10.1002/mrd.10389.
14. Tsujii, H., et al. "The Beneficial Effect of Fructose and Glucose on in Vitro Maturation and the Fertilization of Porcine Oocytes." *Reproductive Medicine and Biology*, vol. 8, Jan. 2009, pp. 19–24. *ResearchGate*, doi:10.1007/s12522-008-0003-8.

15. "6.3 Quadrupole Mass Spectrometers (QMS)." N.p., n.d. Web. 25 May 2017.
<<https://www.pfeiffer-vacuum.com/en/know-how/mass-spectrometers-and-residual-gas-analysis/quadrupole-mass-spectrometers-qms/quadrupole-mass-filter/>>
16. Douglas, D. J. "Linear Quadrupoles in Mass Spectrometry." *Mass Spectrometry Reviews*, vol. 28, no. 6, Nov. 2009, pp. 937–960. *Wiley Online Library*, doi:10.1002/mas.20249.
17. Märk, Tilmann D., and Gordon H. Dunn, editors. *Electron Impact Ionization*. Springer Vienna, 1985.
CrossRef, doi:10.1007/978-3-7091-4028-4.
18. Poole, C. F. *Gas Chromatography*. 2012.
19. "Silylation Derivatization Reagent." *Sigma-Aldrich*. N.p., n.d. Web. 21 May 2017.
<<http://www.sigmaaldrich.com/analytical-chromatography/analytical-reagents/derivatization-reagents/silylation.html>>
20. Huang, Xiaodong, and Fred E. Regnier. "Differential Metabolomics Using Stable Isotope Labeling and Two-Dimensional Gas Chromatography with Time-of-Flight Mass Spectrometry." *Analytical Chemistry* 80.1 (2008): 107–114.
21. Villas-Bôas, Silas G. et al. "Alkylation or Silylation for Analysis of Amino and Non-Amino Organic Acids by GC-MS?" *Metabolites* 1.1 (2011): 3–20. *www.mdpi.com*. Web.
22. Yu, Ran et al. "An Optimized Two-Step Derivatization Method for Analyzing Diethylene Glycol Ozonation Products Using Gas Chromatography and Mass Spectrometry." *Journal of Environmental Sciences* 53 (2017): 313–321.
23. Nikel, P. I., et al. "Pseudomonas Putida KT2440 Strain Metabolizes Glucose through a Cycle Formed by Enzymes of the Entner-Doudoroff, Embden-Meyerhof-Parnas, and Pentose Phosphate Pathways." *The Journal of Biological Chemistry*, vol. 290, no. 43, Oct. 2015, pp. 25920–25932.
doi:10.1074/jbc.M115.687749.

24. Sauer, Uwe. "Metabolic Networks in Motion: ¹³C-Based Flux Analysis." *Molecular Systems Biology*, vol. 2, Nov. 2006, p. 62. *PubMed Central*, doi:10.1038/msb4100109.
25. "HumanCyc: Encyclopedia of Human Genes and Metabolism." N.p., n.d. Web. 13 July 2017
26. Chang, Chih-Hao, et al. "Posttranscriptional Control of T Cell Effector Function by Aerobic Glycolysis." *Cell*, vol. 153, no. 6, June 2013, pp. 1239–51. doi:10.1016/j.cell.2013.05.016.
27. Vander Heiden, M. G., et al. "Understanding the Warburg Effect: The Metabolic Requirements of Cell Proliferation." *Science*, vol. 324, no. 5930, May 2009, pp. 1029–33. *CrossRef*, doi:10.1126/science.1160809.
28. Sriram, G. et al. "Metabolic Flux Maps of Central Carbon Metabolism in Plant Systems." *Concepts in Plant Metabolomics*, edited by Basil J. Nikolau and Eve Syrkin Wurtele, Springer Netherlands, 2007, pp. 125–44. *CrossRef*, doi:10.1007/978-1-4020-5608-6_9.